



Study:

Thermal Emissions of the
Submarine Cable Installation
Viking Link
in the German AWZ

Date: 29.01.2017

client:

IFAÖ GmbH, Rostock

Prof. Dr.-Ing. H. Brakelmann
BCC Cable Consulting
Schwalbenweg 8
47495 Rheinberg

Dr.-Ing. Jörg Stammen
Drüenstraße 12
47506 Neukirchen-Vluyn

Rheinberg und Neukirchen-Vluyn, January 2017

Thermal Emissions of the Submarine Cable Installation Viking Link in the German AWZ

Table of contents

1	Introduction	3
1.1	Project	3
1.2	Thermal emissions study	3
2	Cable Description and Ambient Conditions.....	4
2.1	Technical Data of the Cables.....	4
2.2	Material Parameters of the Cables.....	6
2.3	Parameters of the Seabed.....	6
3	Coupled Eddy Current and Thermal Computations in the Steady State	9
4	Computation of Various Submarine Cables.....	10
4.1	Finite Element Models:	11
4.2	Computational Results.....	13
5	Expansion of the basis of results by means of the LCM-method.....	18
5.1	Summary of the fundamental equations	18
5.2	Further Results.....	21
5.2.1	Case 1a: XLPE-cable 1800 mm ² Cu-conductor, 2 cables in one trench.....	21
5.2.2	Case 1b: XLPE-cable 1800 mm ² Cu-conductor, 1 cable in one trench	22
5.2.3	Case 2a: XLPE-cable 1600 mm ² Cu-conductor, 1 cable in one trench.....	23
5.2.4	Case 2b: XLPE-cable 1600 mm ² Cu-conductor, 2 cables in one trench	24
5.2.5	Case 3a: XLPE-cable 2500 mm ² Al-conductor, 2 cables in one trench	25
5.2.6	Case 3b: XLPE-cable 2500 mm ² Al-conductor, 1 cable in one trench	26
5.2.7	Case 4a: XLPE-cable 2000 mm ² Al-conductor, 1 cable in one trench	27
5.2.8	Case 4b: XLPE-cable 2000 mm ² Al-conductor, 2 cables in one trench	28
5.2.9	Case 5a: MIND-cable 2000 mm ² Cu-conductor, 2 cables in one trench	29
5.2.10	Case 5b: MIND-cable 2000 mm ² Cu-conductor, 1 cable in one trench.....	30
5.2.11	Case 6a: MIND-cable 1800 mm ² Cu-conductor, 1 cable in one trench.....	31
5.2.12	Case 6b: MIND-cable 1800 mm ² Cu-conductor, 2 cables in one trench.....	32
6.	Summary	33
7	Annex	35
7.1	References	35
7.2	Publication: Current rating analysis for cable installations with temperature restrictions	36

1 Introduction

1.1 Project

National Grid Viking Link Limited (NGVL) and Energinet.dk are projecting a new High Voltage Direct-Current (HVDC) submarine transmission line between Great Britain and Denmark, known as Viking Link (Fig. 1), which will be connected with the existing Danish and British onshore transmission systems. Viking Link will be operated with a nominal voltage of 525 kV and with a maximum load of 1.400-MW. It will be connected with the transmission systems Bicker Fen in the county Lincolnshire, Great Britain, and Revising in the southern part of Jutland in Denmark. Viking Link will cross the territorial waters of The Netherlands and of Germany.



Fig. 1: Planned route of the Viking Link

Viking Link has a total length of approx. 760 km and is expected to be operational in 2022. The technical project Viking Link is composed by submarine cables and onshore cables, as well (optionally equipped with optical fibre cables), which are connected with converter stations in Great Britain and in Denmark, thus enabling the power exchange between the both countries in both directions.

The offshore-part of the route consists of two single-core submarine cables, which are laid into the seabed and which will transmit direct current over a length of 630 km between the coasts of Great Britain and Denmark. The offshore cable route is crossing the exclusive economic zones (AWZ) of Great Britain, The Netherlands, Germany and Denmark. The onshore cable route in the British part has a length of approx. 55 km, and in the Danish part of approx. 75 km.

1.2 Thermal emissions study

As a part of the approval procedure the BSH (“Bundesamt für Seeschifffahrt und Hydrographie”, respectively “Federal Maritime and Hydrographic Agency”) requires an analysis of the 2 K-criterion. This study evaluates the 2 K--criterion for several cable configurations in the German AWZ

The calculations shall be performed by a FEM software (FEM – finite-element method) especially designed to compute electromagnetic and thermal fields of cable systems [Sta2001]. Consideration of the mutual influence between conductors, lead sheaths, and armor is enabled by means of magnetic-thermally coupled numerical field analysis, which is able to take the temperature-dependencies of the materials. These FEM-simulations are supplemented by analytic formulations, which are following the IEC-standards.

2 Cable Description and Ambient Conditions

For the Viking link two types of submarine cables with various conductor cross sections are taken into account: cables with an XLPE – (cross-linked polyethylene) insulation and cables with a MIND-insulation (MIND - mass impregnated insulation, non-draining compound).

2.1 Technical Data of the Cables

Fig. 2 a) and b) are showing the structure of the two types of HVDC-submarine cables:

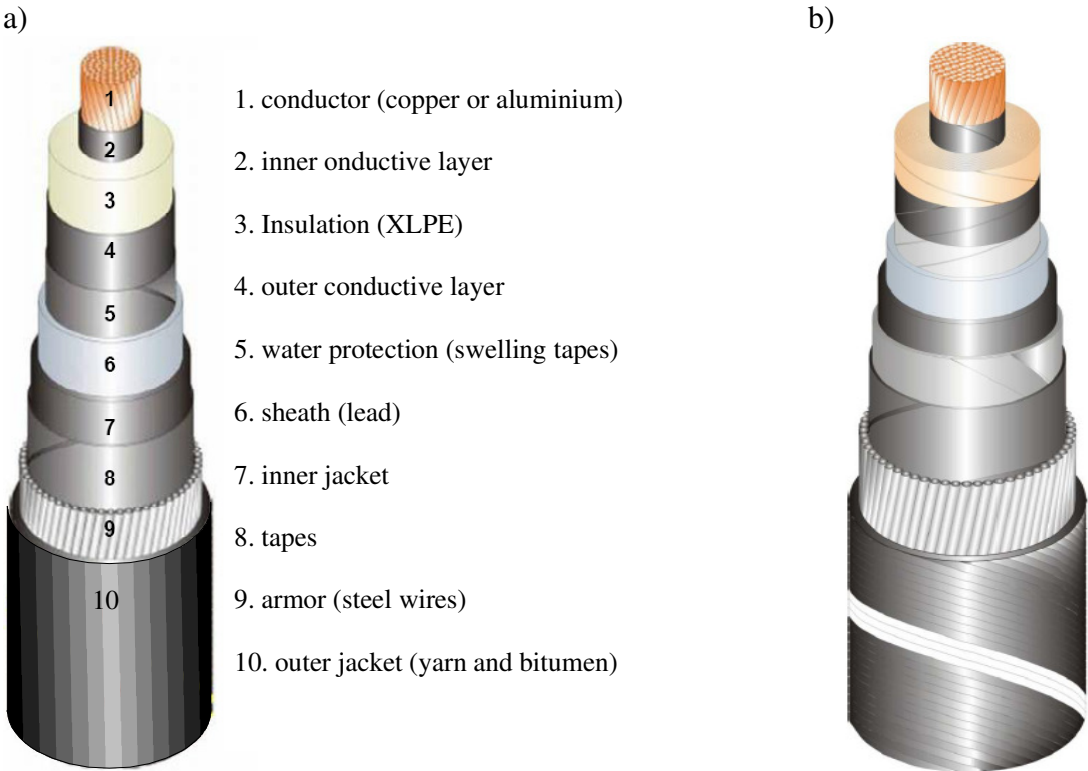


Fig. 2: a) structure of a XLPE-insulated HVDC-submarine cable and b) of a MIND-insulated HVDC-submarine cable (source: ABB)

The assumptions regarding the technical data of the 525-kV-XLPE-cable are listed in Tab. 1:

Stranded conductor	1600 mm ² : 47.6 mm 1800 mm ² : 50.5 mm 2000 mm ² : 53.2 mm 2500 mm ² : 59,5 mm
Thickness of inner conductive layer	1.8 mm
Insulation thickness	26.0 mm
Thickness of outer conductive layer	2.0 mm
Tape	0.5 mm
Lead sheath	5.0 mm
Inner PE jacket	5.0 mm
Tape	0.5 mm
Armour	7.0 mm
Outer jacket	5.0 mm

Tab. 1: Technical data of the 525-kV-submarine cable with XLPE insulation

For the 525-kV-MIND-cable the technical data listed in Tab. 2 has been assumed:

Stranded conductor	1800 mm ² : 50.5 mm 2000 mm ² : 53.2 mm
Thickness of inner conductive layer	1.2 mm
Insulation thickness	22.0 mm
Thickness of outer conductive layer	2.5 mm
Tape	0.5 mm
Lead sheath	5.0 mm
Inner PE jacket	5.0 mm
Tape	0.5 mm
Armor	7.0 mm
Outer jacket	5.0 mm

Tab. 2: Technical data of the 525-kV-submarine cable with MIND insulation

Please note that for all conductor cross sections the same conductor diameter and the same wall thicknesses for the insulation, for the conductive layers, for the lead sheaths as well as for the armour and the outer jacket are chosen. The reason is that the six cables are not specified by the client or by a provider in detail at the moment. In this context, one should keep in mind that these constructional details are of some importance for the current rating of

the cables, but that they have a negligible influence on the temperature rise of the survey point in the seabed.

For the cases with two cables in the trench it is assumed that the both cables touch each other. For the cases with a single cable in the trench the laying distance to the second cable is large enough that a mutual heating can be neglected, i.e. for example more than 20 m.

2.2 Material Parameters of the Cables

In the following section the material parameters used for the cable are specified.

Meaning of the symbols: λ thermal conductivity, c heat capacity, ρ density, κ specific electrical conductivity, and α temperature coefficient.

Conductor:

a) Copper

Round compacted copper wires, $\lambda = 372 \text{ W/mK}$, $c = 385 \text{ Ws/kgK}$, $\rho = 8900 \text{ kg/m}^3$, $\kappa = 58 \cdot 10^6 \text{ 1/}\Omega\text{m}$, $\alpha = 3,93 \cdot 10^{-3} \text{ 1/K}$ (el. conductivity will be modified by a fill factor of 0.90).

b) Aluminium

Round compacted aluminium wires, $\lambda = 237 \text{ W/mK}$, $c = 897 \text{ Ws/kgK}$, $\rho = 2707 \text{ kg/m}^3$, $\kappa = 35 \cdot 10^6 \text{ 1/}\Omega\text{m}$, $\alpha = 4,03 \cdot 10^{-3} \text{ 1/K}$, (fill factor 0.9).

Insulation:

XLPE, $\lambda = 0.2857 \text{ W/mK}$, $c = 2300 \text{ Ws/kgK}$, $\rho = 930 \text{ kg/m}^3$.

Tapes:

Fleece, $\lambda = 0.166 \text{ W/mK}$, $c = 1700 \text{ Ws/kgK}$, $\rho = 2680 \text{ kg/m}^3$.

Lead sheaths:

Lead alloy, $\kappa = 4.8 \cdot 10^6 \text{ 1/}\Omega\text{m}$, $\lambda = 35.3 \text{ W/mK}$, $c = 129 \text{ Ws/kgK}$, $\rho = 11340 \text{ kg/m}^3$

Jacket:

Polyethylene, $\lambda = 0.40 \text{ W/mK}$, $c = 2274.9 \text{ Ws/kgK}$, $\rho = 1055 \text{ kg/m}^3$

Armour:

steel wires, $\kappa = 6,9 \cdot 10^6 \text{ 1/}\Omega\text{m}$, $\alpha = 4,5 \cdot 10^{-3} \text{ 1/K}$, $\lambda = 47 \text{ W/mK}$, $c = 490 \text{ Ws/kgK}$, $\rho = 7800 \text{ kg/m}^3$.

2.3 Parameters of the Seabed

Usually the soil of the seabed is assumed to be homogeneous with a constant thermal conductivity. No partial dry-out of the soil (which is mandatory for land cable routes) is assumed, on the contrary a permanent humidification of the soil pores can be ensured. Hence, one can say the soil of the seabed is water saturated.

The seabed's soil mainly consists of sand, gravel, clay glacial drift and silt. The thermal conductivities of these components according to [Smo2001] are given in Tab. 3:

Thermal properties of water-saturated soils [Smo2001]	Min. thermal conductivity	Max. thermal conductivity	Max. specific thermal resistance	Min. specific thermal resistance
	W/(K m)	W/(K m)	K m/W	K m/W
Kies / gravel	2.00	3.30	0.50	0.30
Sand	1.50	2.50	0.67	0.40
Ton / clay	0.90	1.80	1.11	0.56
Geschiebemergel / glacial drift	2.60	3.10	0.38	0.32
Schluff/Schlick / silt	1.4	2.00	0.71	0.50

Tab. 3: Thermal properties of water-saturated soils [Smo2001]

Due to Tab. 3 a maximum thermal resistance of 0.7 Km/W can be derived. This complains with measurements [Wal2003] while planning the Viking-Cable's cable route.

- German coast of the North Sea $\rho = 0.7 \text{ Km/W}$
- North Sea coast of Denmark and Belgium $\rho = 0.6 \text{ Km/W}$






In [Bar1977] the following thermal resistivities of the seabed's soil for installed submarine cable routes are given, which in one case are somewhat higher (0.9) :

- United Kingdom - France $\rho = 0.7 \text{ K m/W}$
- Denmark - Sweden $\rho = 0.9 \text{ K m/W}$
- Br. Columbia-Vancouver Island $\rho = 0.7 \text{ K m/W}$
- Long Island Sound $\rho = 0.7 \text{ K m/W}$

Looking into a report about measurements along the cable route ([FUG2016], about the by far greatest part of the route we find much higher values. Wherever in some few points "anomalous values" are given, which are slightly undergoing a value of $\lambda = 1.43 \text{ W/(K m)}$, this happens in a thin layer of soil, and these points are immediately neighbored by regions with thermal conductivities, which are by far higher. Under thermal aspects, these singular and severely limited points are not expected to be relevant. This is the reason that in the following a value of $\lambda = 1.43 \text{ W/(K m)}$ (i.e. $\rho = 0.70 \text{ W/(K m)}$) will be adopted here. This is according to the assumptions in other studies about cable routes crossing the North Sea, as for windfarm export cables in [Bra2004], [Bra2010], [Fri2010] and a lot of others, thus following the advice of the BSH in [BSH2007].

The water temperatures vary from 3 °C to 17 °C (see Tab. 4), and in [BSH2012] the average water temperature of the North Sea is determined to 9 °C.

Here, again on the safe side, a temperature of 15 °C is assigned to the thermally undisturbed soil as well as to the seabed's surface. Because the seabed's surface is flooded with water it can be considered in the simulations as an ideal heat sink.

	Jan	Feb	März	Apr	Mai	Jun	Jul	Aug	Sep	Okt	Nov	Dez
 Maximal-Temperatur	3°	2°	6°	10°	12°	18°	19°	20°	17°	12°	8°	2°
 Minimal-Temperatur	0°	-1°	0°	4°	8°	11°	14°	14°	12°	8°	4°	4°
 Sonnen-Stunden	2h	3h	4h	6h	7h	9h	8h	7h	5h	3h	2h	2h
 Wasser-Temperatur	4°	3°	5°	6°	10°	13°	17°	17°	16°	13°	9°	6°
 Regentage	12	9	8	8	7	7	9	12	12	13	14	13

Tab. 4: Table of the monthly's average water and air temperatures of the North Sea [Rei2012]

Moreover, the undisturbed temperature of the seabed, here chosen to 15°C, plays a nearly negligible role for the calculation of the temperature rise in the survey point (2 K-criterion).

3 Coupled Eddy Current and Thermal Computations in the Steady State

Ohmic losses, and in the case of AC-transmission eddy current losses and dielectric losses as well as the hysteresis losses in ferromagnetic elements generate heat power which heats up the cable and its environment.

Beside the thermal effects (e.g. drying-out of the soil) the rising temperature also causes a change in the electrical conductivity of the conductors and the sheaths. For example, the resistance of typical conductor material copper or aluminium, increases with the temperature. According to

$$P' = R' \cdot I^2 = \frac{S^2 \cdot A_L}{\kappa}$$

the losses per unit length increase when the electric resistance ρ increase (respectively when the conductivity κ decrease). With S the current density and A_L the conductor cross section and the equation

$$R'(\vartheta) = R'_{20} \cdot (1 + \alpha(\vartheta - 20^\circ\text{C}))$$

the resistance per unit length R' will increase by 19.65 % for a copper conductor ($\alpha_{\text{Cu}} = 3.93 \cdot 10^{-3} \text{ 1/K}$) and by 20.15 % for an aluminium conductor ($\alpha_{\text{Al}} = 4.03 \cdot 10^{-3} \text{ 1/K}$) if the conductor temperature rises up to 70 °C.

Therefore, an iteration of the temperature dependent material properties must be included in the FEM calculation, in order to obtain reliable results. This means an coupled computation of the thermal and magnetic field. At first a current computation is performed at ambient temperature. Then the current losses P' are converted to heat sources for the computation of the thermal field. Temperature dependent material parameters are modified and a new eddy current computation is performed.

The electrical conductivity is modified by:

$$\kappa(\vartheta) = \frac{\kappa(20^\circ\text{C})}{1 + \alpha_{20} \cdot (\Delta\vartheta)}$$

This iterative calculation is repeated until the change of the material parameters is negligible.

4 Computation of Various Submarine Cables

Six different cables (see Tab. 5) are examined with respect to the 2 Kelvin criterion, laying depth and conductor temperature. Altogether 12 cases are considered for the six cables (cases 1a to 6a and 1b to 6b in Tab. 5), which differ in the laying arrangement: “one cable in 1 trench” means, that the second cable is separately laid in a distance of more than 20 m, so that they are thermally decoupled. In the case of “two cables in 1 trench” the two cables are laid in a bundle, i.e. without a clearance between them. For each cable both arrangements are discussed (see definition of cases in Tab. 5).

Viking-Link with two 525 kV-HVDC cables		unit	case 1 cable 1	case 2 cable 2	case 3 cable 3	case 4a cable 4	case 5a cable 5	case 6a cable 6
U_n	nominal voltage	kV	525	525	525	525	525	525
S_{tot}	transmission power, 2 cables	MW	1400	1400	1400	1400	1400	1400
I	current of 1 cable	A	1333	1333	1333	1333	1333	1333
n	number of cables in 1 trench cases 1a to 6a	-	2	1	2	1	2	1
n	number of cables in 1 trench cases 1b to 6b	-	1	2	1	2	1	2
$\Theta_{c,max}$	permissible conductor temperature	°C	70	70	70	70	55	55
A_c	cross section of conductor	mm ²	1800	1600	2500	2000	2000	1800
	conductor material		Cu	Cu	Al	Al	Cu	Cu
α	temperature coefficient	1/K	0.0039	0.0039	0.0043	0.0043	0.0039	0.0039
D_c	outer diameter of conductor	mm	50.5	47.6	59.5	53.2	53.2	50.5
s_1	insulation thickness incl. semiconductive layers	mm	29.8	29.8	29.8	29.8	24.7	24.7
s_{LS}	thickness of lead sheath	mm	5.0	5.0	5.0	5.0	5.0	5.0
s_2	thickness of inner protective layer	mm	5.0	5.0	5.0	5.0	5.0	5.0
s_{Arm}	thickness of armor	mm	7.0	7.0	7.0	7.0	7.0	7.0
s_3	thickness of outer protective layer	mm	5.0	5.0	5.0	5.0	5.0	5.0
D	outer diameter of the cable	mm	145	142	153	147	137	134
ρ_{th1}	spec. thermal resistivity of el. insulation	K m/W	3.5	3.5	3.5	3.5	6.0	6.0
ρ_{th2}	spec. thermal resistivity of inner protective layer	K m/W	6.0	6.0	6.0	6.0	6.0	6.0
ρ_{th3}	spec. thermal resistivity of outer protective layer	K m/W	6.0	6.0	6.0	6.0	6.0	6.0
h_c	laying depth (cover. 1.50 m)	m	1.57	1.57	1.58	1.57	1.57	1.57
h_p	depth of the survey point	m	0.20	0.20	0.20	0.20	0.20	0.20
Θ_{amb}	ambient temperature	°C	15	15	15	15	15	15
λ	thermal conductivity of soil	W/(K m)	1.43	1.43	1.43	1.43	1.43	1.43
$\Delta\Theta_{p,m}$	permissible temperature rise of survey point P	K	2.0	2.0	2.0	2.0	2.0	2.0

Tab. 5: Parameters of the six cables and 12 cases

For the interpretation of Tab. 5, one has to keep in mind that at this point of time the dimensions of the cables are not really fixed in detail. This will be done in the latest planning step, based on the constructional details in the tenders of the cable manufacturers. On the other hand, such constructional details – as e.g. slightly deviating wall thicknesses of the electrical insulation, armour, sheaths etc. – are (for HVDC-cables) of negligible importance for the temperature rise in the survey point. This temperature rise is mainly governed by the conductor losses (i.e. by current, cross section and material of the conductor) and by the coordinate of the conductor's axis.

As an example, the wall thickness of the electrical insulation of cable 2, case 2a, of the following scenarios (XLPE-cable, 1600 mm² copper conductor, 1.5 m covering depth) was changed by 5 mm from 26 mm to 31 mm: results were deviations of the temperature rise in the survey point by less than 2 per mill.

The following calculations are based on a steady-state operation, which means a load factor of $m = 1.0$ for the transmission of electrical energy for such a long time, that all warming up processes are terminated. It should be clear that this is an extremely conservative approach. In the following section the Finite-Element model, matching this approach, will be described.

4.1 Finite Element Models:

For each conductor cross section a new finite-element model has been created. The following figures (Fig. 3 to Fig. 5) show the finite-element model of case 1a as an example of two cables (1800 mm² Cu) in one trench. Since the discretization in the area of the cable is very fine, enlarged details of the model are shown in some extra pictures.

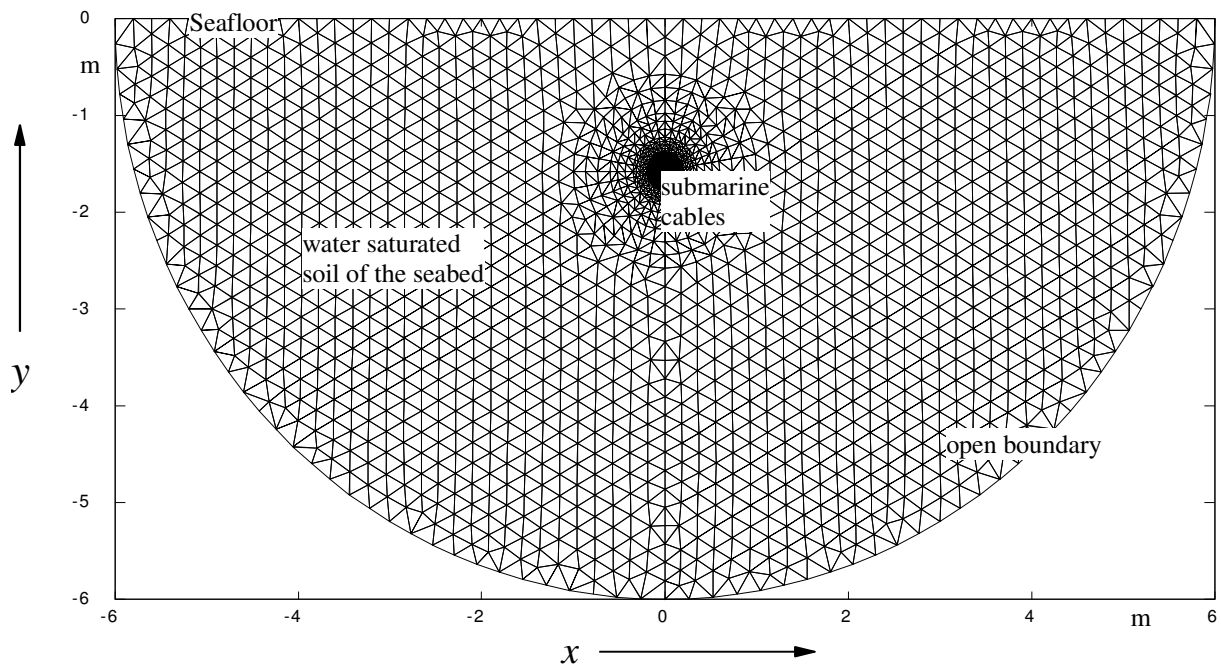


Fig. 3: Finite-element model

The surrounding soil is implemented as a finite element model up to a circular rim which represents a so-called "open boundary". Here the temperatures are not set to a constant value

rather the thermal field can decay to the undisturbed ambient temperature in the infinity. Thus the numerical errors of boundaries with fixed values are avoided. The seabed's surface is - as explained in section 2.3 - a heat sink set to a temperature of 15 °C. The undisturbed ambient temperature is assumed to be 15 °C.

The results of the computations are given and discussed in the next section (section 4.2).

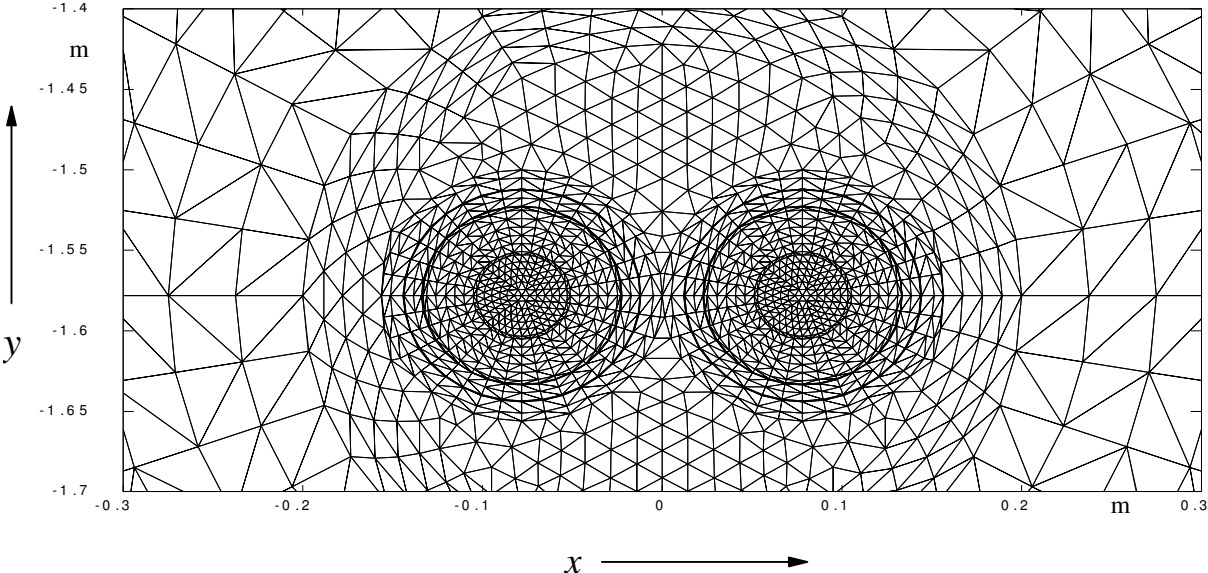


Fig. 4: Details of the finite-element model in the area of the submarine cable, XLPE, case 1a, 1800 mm² Cu, two cables in one trench

Also the case of only one cable in a trench (e.g. case 2a) has to be considered in this study. Fig. 5 shows a part of the finite element model for case 2a - the XLPE insulated cable (1600 mm² copper) with some highlighted structure of the cable.

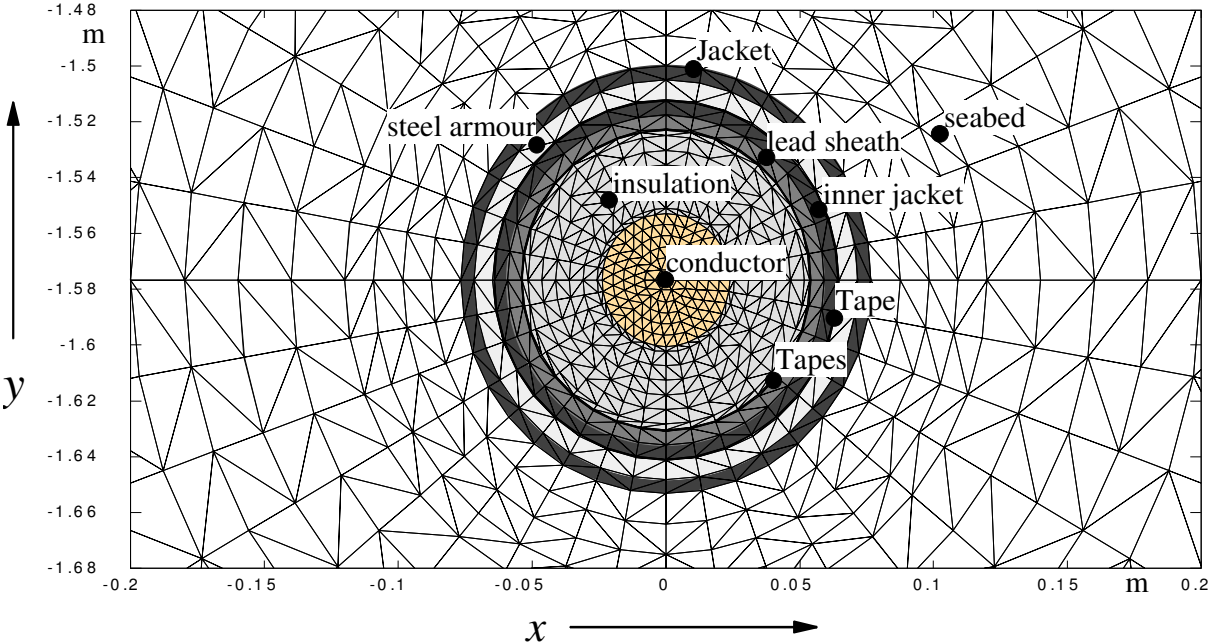


Fig. 5: Details of the finite-element model in the area of the submarine cable, XLPE, 1600 mm² Cu, one cable in the trench

4.2 Computational Results

Fig. 6 shows the temperature distribution for case 1a within and around the 1800 mm² Cu-submarine cables with XLPE insulation at a laying depth of 1.50 m (measured from the seafloor to the top of the cables). The temperature scale indicates that the conductor temperature of 39.0°C (color red) is well below the maximum temperature of 70 °C.

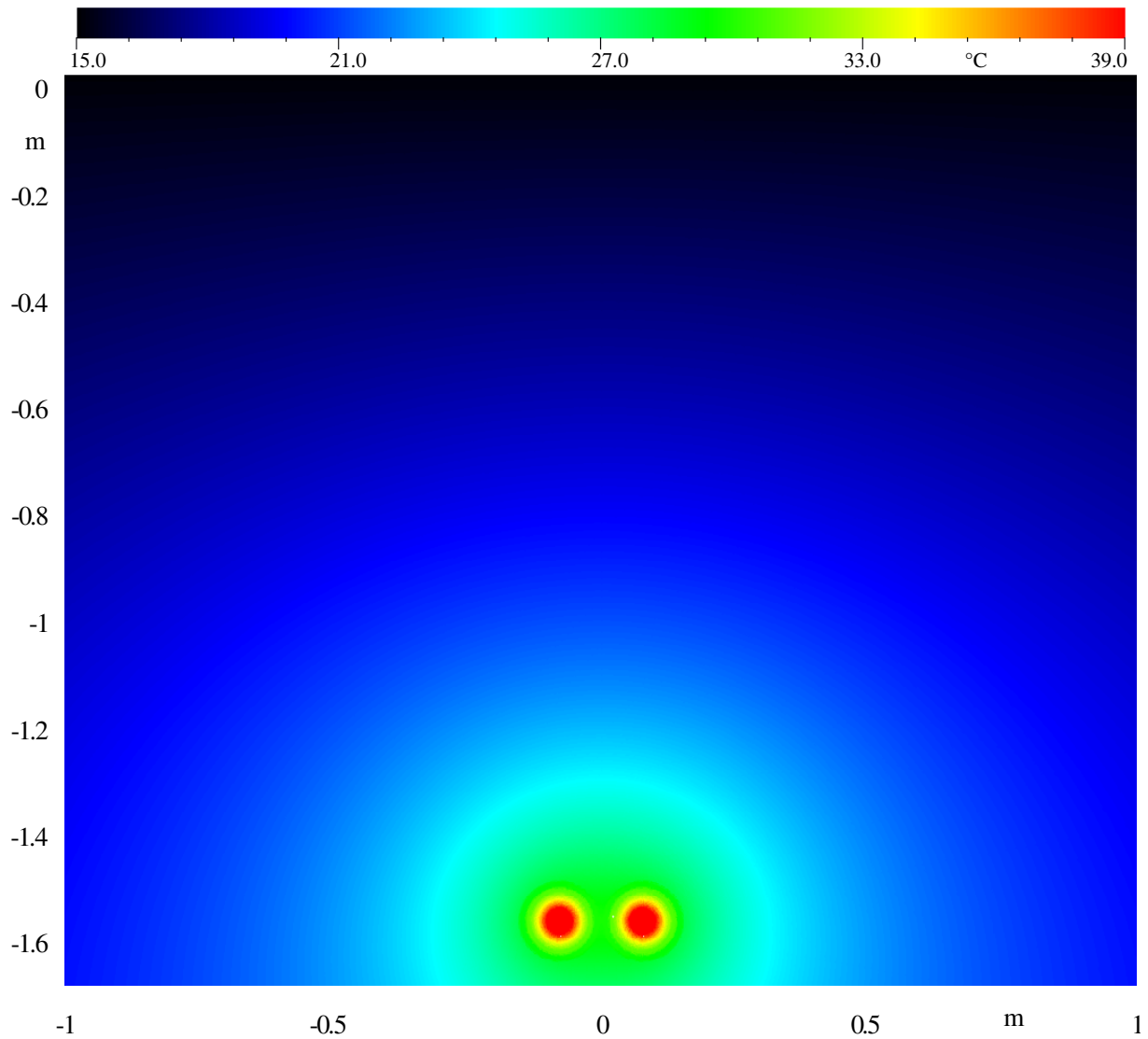


Fig. 6: Temperature distribution within and around the two submarine cables (1800 mm² Cu) for a continuous load of 1333 A, case 1a: two cables in one trench; the distance of the cables axes is identical with the cable diameter of 145 mm; 2x1333 A

The next diagram (Fig. 7) shows the same temperature distribution but in three dimensions:

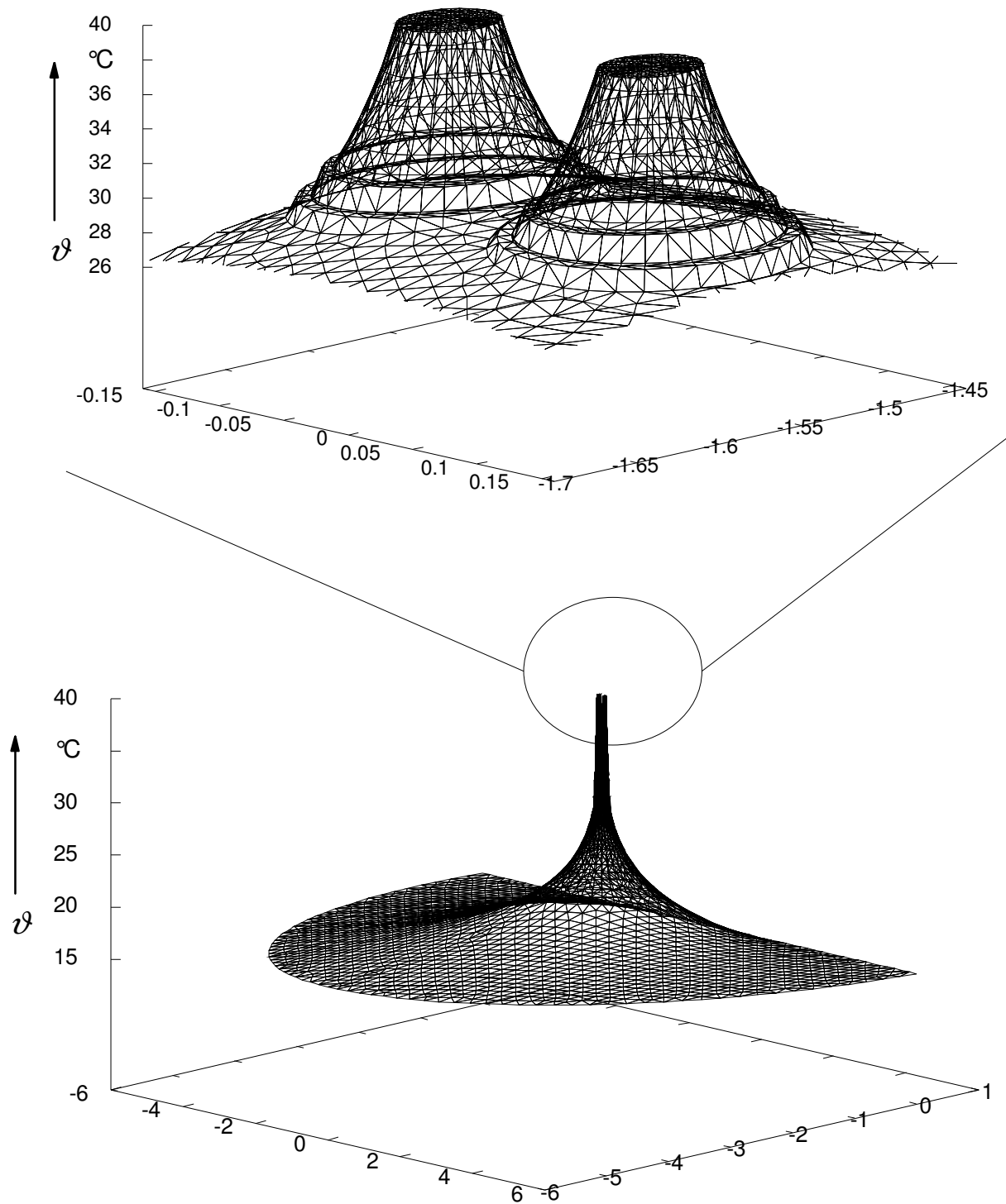


Fig. 7: Temperature distribution within and around the submarine cables ($1800 \text{ mm}^2 \text{ Cu}$) for a continuous load of 1333 A, case 1a: two cables in one trench; $2 \times 1333 \text{ A}$

As another example, the following Fig. 8 shows the temperature distribution for case 2a within and around the submarine cable ($1600 \text{ mm}^2 \text{ Cu}$) with XLPE insulation at a laying depth of 1.5 m, here only with a single cable in the trench. The temperature scale shows that the conductor temperature is only 35.5°C .

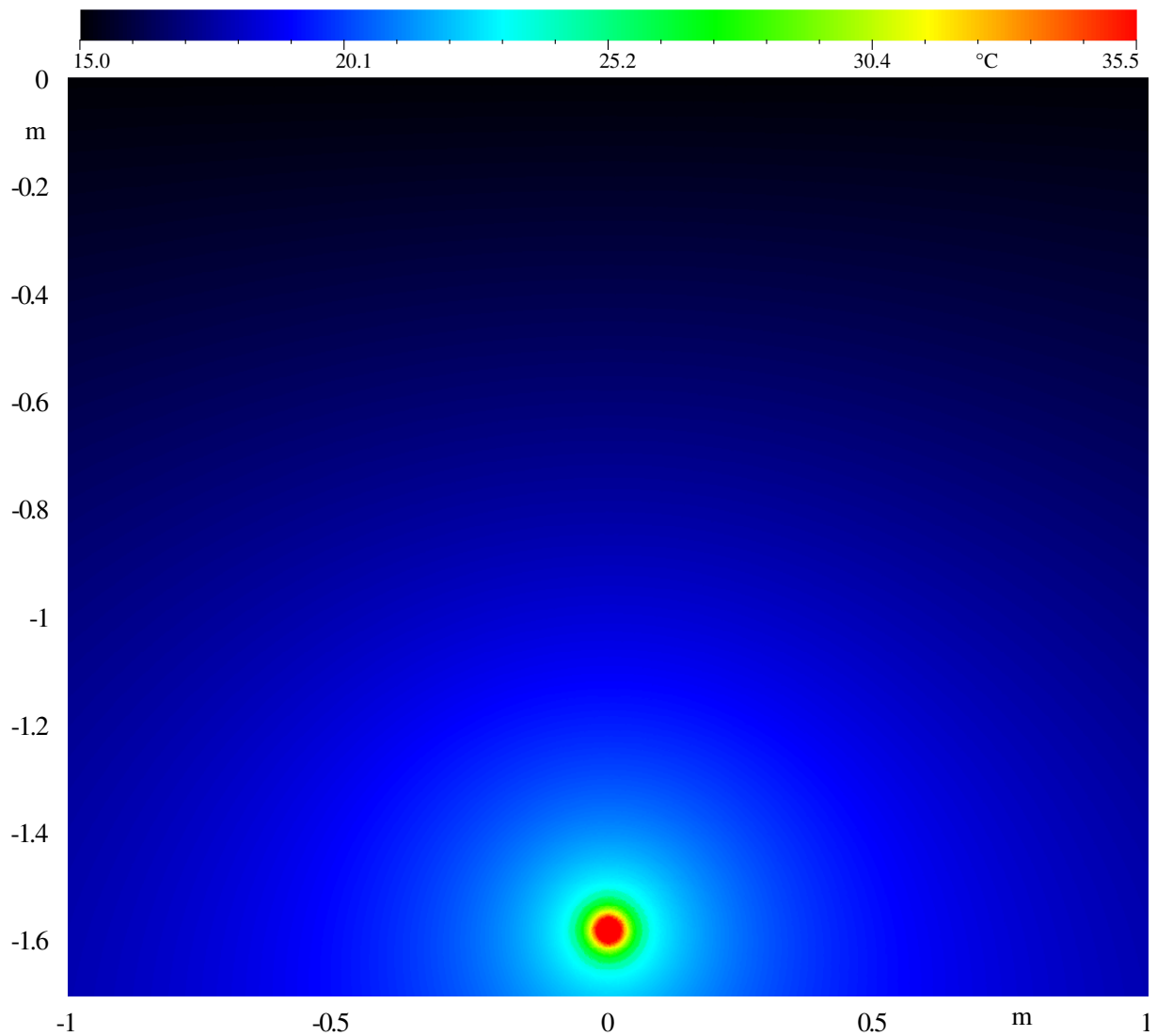


Fig. 8: Temperature distribution within and around the submarine cable (1600 mm² Cu) for a continuous load of 1333 A, case 2a: one cables in the trench, distance to the second cable > 20 m; 2x1333 A;

The finite element method provides a continuous temperature distribution of the whole discretized area. The diagrams above are suited to see the temperature distribution at a glance. But to examine the temperature distribution in detail e.g. at a depth of 0.2 m beyond the seafloor, horizontal line scans are the best choice.

Fig. 9 shows line scans of the two examples above. The maximum temperature at the survey point is 16.03°C in the case of two XLPE-cables with a copper cross section of 1800 mm² and 15.58°C in the case of one XLPE-cable with a copper cross section of 1600 mm². Taking the ambient temperature of 15 °C into account, we have temperature rises of 1.03 K for the 1800 mm² conductors and of 0.58 K for the 1600 mm² conductors, respectively.

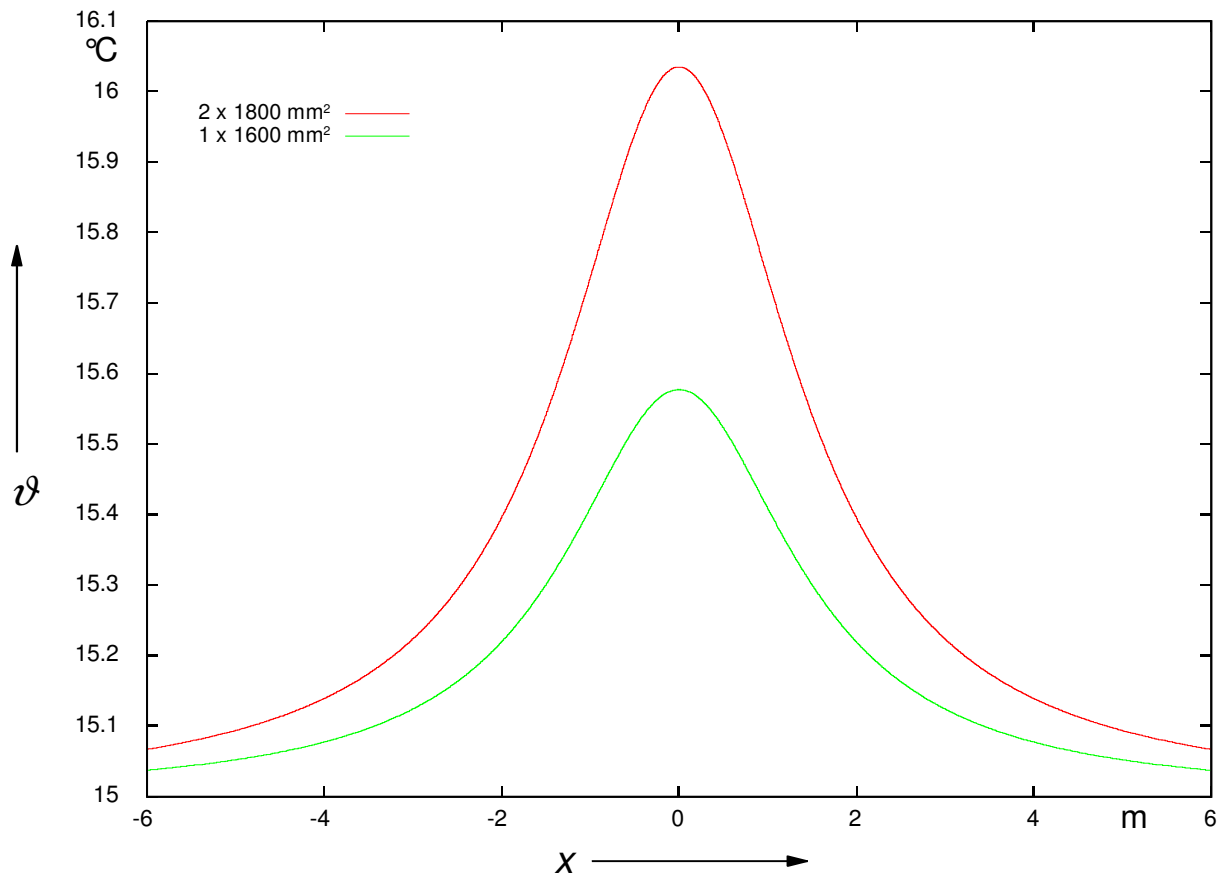


Fig. 9: Temperature line scan within at a depth of 0.2 m in the soil for the both 1800 mm² submarine cables (case 1a) and for the single 1600 mm² submarine cable (case 2a), continuous load 1333 A

These temperature line scans have been performed for all six cables and all twelve cases, respectively. Furthermore, the laying depths have been minimized in steps of 5 cm with the aim to approach closely a temperature rise of 2 K. The results are summarized in Tab. 6.

HVDC cable 525 kV		$\Delta\Theta_{P,1.5m}$	$\Theta_{c,1.5m}$	$\Theta_{S,1.5m}$	$h_{c,min}$	$\Theta_{c,min}$	$\Theta_{S,min}$
case	cable	K	°C	°C	m	°C	°C
1a	XLPE 1800 Cu 2 cables	1.03	39.0	28.3	0.75	36.2	25.5
1b	XLPE 1800 Cu 1 cable	0.51	32.6	22.3	0.40	30.1	19.8
2a	XLPE 1600 Cu 1 cable	0.58	35.5	23.4	0.45	32.8	20.7
2b	XLPE 1600 Cu 2 cables	1.18	43.0	30.2	0.85	40.3	27.7
3a	XLPE 2500 Al 2 cables	1.21	41.7	30.3	0.90	39.3	27.9
3b	XLPE 2500 Al 1 cable	0.59	34.3	23.4	0.45	31.6	20.7
4a	XLPE 2000 Al 1 cable	0.76	40.8	25.9	0.55	37.8	23.0
4b	XLPE 2000 Al 2 cables	1.57	50.9	35.0	1.15	49.1	33.3
5a	MIND 2000 Cu 2 cables	0.94	40.9	27.1	0.70	38.0	24.3
5b	MIND 2000 Cu 1 cable	0.46	34.9	21.7	0.35	32.4	19.2
6a	MIND 1800 Cu 1 cable	0.52	37.4	22.5	0.40	34.8	20.0
6b	MIND 1800 Cu 2 cables	1.06	44.3	28.8	0.75	41.4	26.9

Tab. 6: Results of the FEM-computations for all six cables and all 12 cases; 2x1333 A; $\lambda = 1.43$ W/(K m)

Legend:

- $\Delta\Theta_{P,1.5m}$ temperature rise of survey point for coverage depth of 1.5 m
- $\Theta_{c,1.5m}$ conductor temperature for coverage depth of 1.5 m
- $\Theta_{S,1.5m}$ surface temperature for coverage depth of 1.5 m
- $h_{c,min}$ minimal coverage depth for the 2 K-limit
- $\Theta_{c,min}$ conductor temperature for minimal coverage depth
- $\Theta_{S,min}$ surface temperature for minimal coverage depth

5 Expansion of the basis of results by means of the LCM-method

In the preceding sections, the essential results – minimum coverage depth as well as temperature rise of the survey point for a coverage depth of 1.50 m – have been worked out by means of a special FEM-simulation program and presented there. In the following, it is intended to upgrade these results by means of characteristic lines. The LCM-method (line charge method) instead of the FEM-method is used hereby, thus reducing the number of necessary FEM-models. As proven in [BS2006], for isothermal surfaces the results of the LCM-method are comparable to those of the FEM-method, which is stated in the BSH-rules [BSH2007], too. By the way, the LCM-method corresponds to the calculation procedures proposed in IEC-publication 60287 [IEC2006], i.e. to the international standards.

Since the mentioned condition of an isothermal surface is well satisfied [BS2006], only inside of the cables small deviations of the heat fluxes can be expected (as compared with FEM). These heat fluxes are considered by the LCM-method by means of thermal resistances well-defined by IEC-publ. 60287. The fundamental equations which are used here will be summarized below. Further explanations, as well for time-dependent load, can be found in the publication of annex 7.2, which was published in December 2016 in the journal “ew”.

5.1 Summary of the fundamental equations

In cable technology, the stationary mutual heating of cables and the temperature rise of other space points is mostly calculated on the basis of IEC-publication 60287 [IEC2006], i.e. by means of the so-called Kenelly-formula, which approximately presents the cable in the soil by two heat-emitting line sources: one of these line sources lies in the cable axis and emits the cables losses (p.u.l.) P' , see Fig. 10. The second one is given by reflection at the soil surface, see Fig. 10, there emitting the negative cables losses (p.u.l.) $-P'$. This arrangement enables to model a system, where the soil surface becomes an isotherm with the temperature rise $\Delta\Theta = 0$ K. From this and for cables losses of P_C' the temperature rise $\Delta\Theta_P$ of a survey point and the mutual thermal resistance T_{CP}' follow with equ. (1).

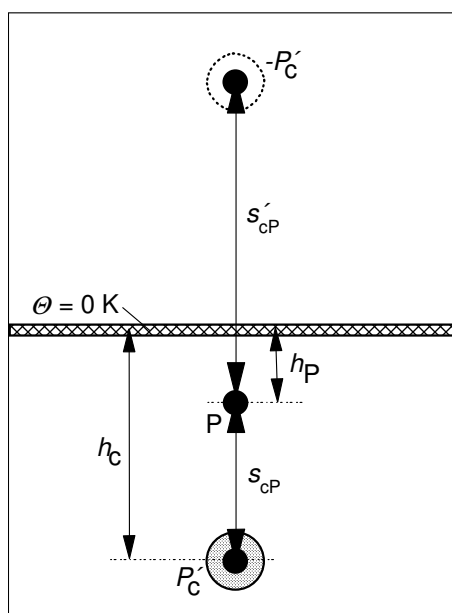


Fig. 10: Determination of the temperature rise $\Delta\Theta_P$ of a survey point by means of the LCM-method for one cable

$$\Delta\theta_P = P' \cdot T'_{CP} = P' \cdot \frac{1}{2 \cdot \pi \cdot \lambda} \cdot \ln \frac{s'_{CP}}{s_{CP}} = P' \cdot \frac{1}{2 \cdot \pi \cdot \lambda} \cdot \ln \frac{h_c + h_p}{h_c - h_p} \quad (1)$$

s_{CP} distance between cable and survey point P and
 s'_{CP} distance between mirrored cable and survey point P.

From this and for a given temperature rise $\Delta\theta_P$ of the survey point, the permissible cable losses follow:

$$P'_{\max,2K} = \frac{\Delta\theta_P}{T'_{CP}} = \frac{1 + \alpha \cdot (\theta_c - 20^\circ C)}{\kappa_{20} \cdot A} \cdot I^2 \quad (2)$$

where A cross section of the conductor,
 I load current,
 κ_{20} el. conductivity of the conductor material for 20°C and
 α temperature coefficient.

With the conductor temperature θ_c

$$\theta_c - \theta_a = R_{c,20} \cdot [1 + \alpha \cdot (\theta_c - 20^\circ C)] \cdot I^2 \cdot (T'_1 + T'_2 + T'_3 + T'_4) \quad (3)$$

where θ_a ambient temperature and
 $R_{c,20} = 1/(\kappa_{20} A)$ el. resistance of the conductor (20°C, p.u.l.).

T'_1, T'_2, T'_3 are the thermal resistances of the inner layers of the cable (insulation etc.), for which we get in the present coaxial case (inner radius r_i , outer radius r_a , thermal conductivity λ):

$$T'_i = \frac{1}{2 \cdot \pi \cdot \lambda} \cdot \ln \frac{r_{a,i}}{r_{i,i}} \quad (4)$$

The external thermal resistance of the cable (external diameter D) is

$$T'_4 = \frac{1}{2 \cdot \pi \cdot \lambda} \cdot \ln \frac{4 \cdot h_c}{D} \quad (5)$$

Modifying Gl. (3) yields the conductor temperature as

$$\theta_c = \frac{R_{c,20} \cdot [1 - \alpha \cdot 20^\circ C] \cdot I^2 \cdot (T'_1 + T'_2 + T'_3 + T'_4) + \theta_a}{1 - \alpha \cdot R_{c,20} \cdot I^2 \cdot (T'_1 + T'_2 + T'_3 + T'_4)} \quad (6)$$

For the case of two closely neighbored cables (Fig. 11) we get the following derivation with the equations (7) to (11), which are equivalent to the preceding equations (1) to (6):

$$\Delta\theta_P = 2 \cdot P' \cdot T'_{CP} = 2 \cdot P' \cdot \frac{1}{4 \cdot \pi \cdot \lambda} \cdot \ln \frac{\Delta x^2 + (h_c + h_p)^2}{\Delta x^2 + (h_c - h_p)^2} \quad (7)$$

$$P'_{\max,2K} = \frac{\Delta\theta_p}{2 \cdot T'_{CP}} = \frac{1 + \alpha \cdot (\theta_c - 20^\circ\text{C})}{\kappa_{20} \cdot A} \cdot I^2 \quad (8)$$

with

$$\theta_c - \theta_a = R_{c,20} \cdot [1 + \alpha \cdot (\theta_c - 20^\circ\text{C})] \cdot I^2 \cdot (T'_1 + T'_2 + T'_3 + T'_4) \quad (9)$$

where

$$T'_4 = \frac{1}{4 \cdot \pi \cdot \lambda} \cdot \ln \left\{ \left(\frac{4 \cdot h}{D} \right)^2 \cdot \left[1 + \left(\frac{2 \cdot h}{s} \right)^2 \right] \right\} \quad (10)$$

The conductor temperature follows as:

$$\theta_c = \frac{R_{c,20} \cdot [1 - \alpha \cdot 20^\circ\text{C}] \cdot I^2 \cdot (T'_1 + T'_2 + T'_3 + T'_4) + \theta_a}{1 - \alpha \cdot R_{c,20} \cdot I^2 \cdot (T'_1 + T'_2 + T'_3 + T'_4)} \quad (11)$$

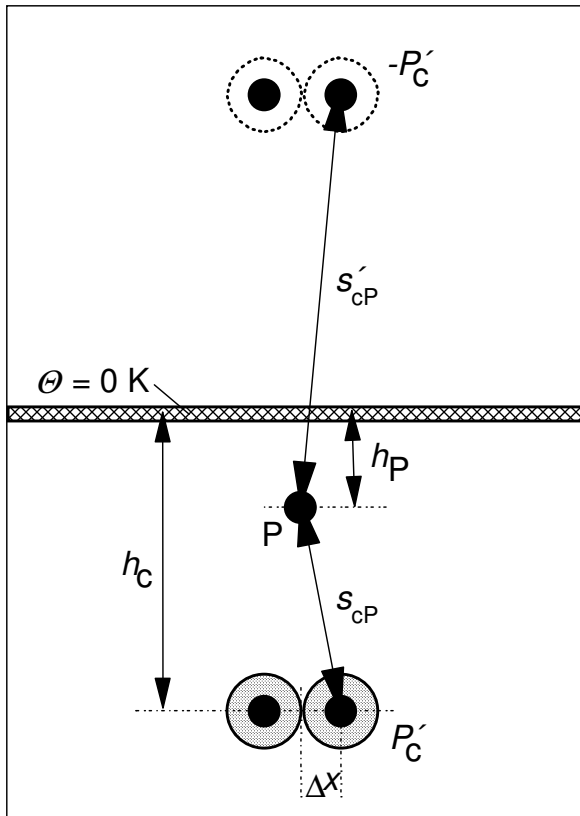


Fig. 11: Determination of the temperature rise $\Delta\theta_p$ of a survey point by means of the LCM-method for 2 cables

5.2 Further Results

By means of the before derived fundamental equations, in the following some results for the discussed twelve cases are summarized below. To this, for a given current of 1333 A for each cable the figures (Fig. 12 to Fig. 23) show the temperature rise of the survey point $\Delta\Theta_P$ as well as the conductor temperature Θ_c . A thermal conductivity of the seabed of $\lambda = 1.0 \text{ W/(K m)}$ and a temperature of the undisturbed soil of $\Theta_{\text{amb}} = 15^\circ\text{C}$ are assumed again. For comparison with the FEM-simulations, blue triangles represent the FEM-results, which in all cases are in excellent consistency with the results of the LCM-method.

5.2.1 Case 1a: XLPE-cable 1800 mm² Cu-conductor, 2 cables in one trench

For this case 1a of Tab. 5 and Tab. 6 and for the given current of 1333 A each cable, in Fig. 12 the temperature rise of the survey point $\Delta\Theta_P$ (green) as well as the conductor temperature Θ_c (red) are shown as functions of the laying depth h . The results for a coverage depth of 1.50 m are marked by circles, whereas those for the minimal coverage depth are marked by quadrats. Additionally, the results of the FEM-simulations are recorded by means of blue triangles.

First, the excellent consistency of the LCM-results with the FEM-results becomes obvious. For the planned coverage depth of 1.50 m we get a temperature rise of the survey point of $\Delta\Theta_P = 1.03 \text{ K}$, which is considerably lower than the limit value of 2.0 K. In this case the conductor temperature reaches only 39.0°C , i.e. by far lower than the critical value of 70°C .

The minimal coverage depth of the cable, for which the limit value of 2.0 K will be reached, is 0.75 m. For this, a conductor temperature of 36.2°C is reached.

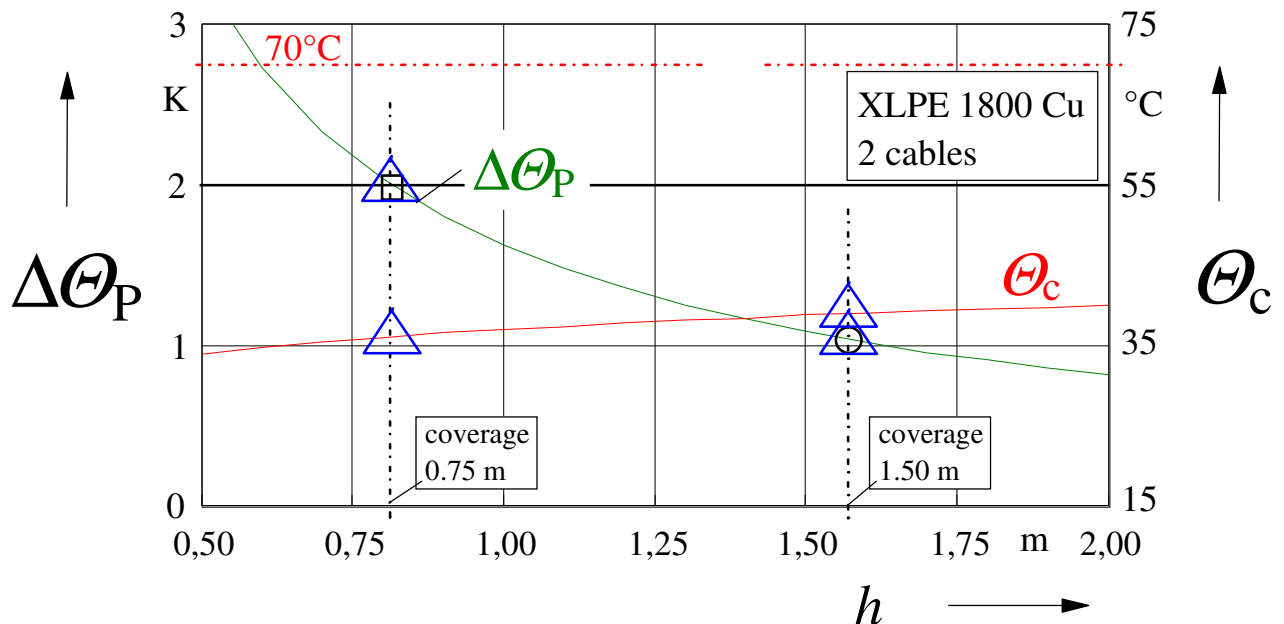


Fig. 12: Temperature rise $\Delta\Theta_P$ of survey point (green) and conductor temperature Θ_c (red) as functions of the laying depth h ; Δ = FEM-result; $\lambda = 1.43 \text{ W/(K m)}$; $\Theta_{\text{amb}} = 15^\circ\text{C}$, Case 1a: XLPE-cable 1800 mm² Cu-conductor, 2 cables in one trench

5.2.2 Case 1b: XLPE-cable 1800 mm² Cu-conductor, 1 cable in one trench

For this case 1b of Tab. 5 and Tab. 6 and for the given current of 1333 A each cable, in Fig. 13 the temperature rise of the survey point $\Delta\Theta_P$ (green) as well as the conductor temperature Θ_C (red) are shown as functions of the laying depth h . The results for a coverage depth of 1.50 m are marked by circles, whereas those for the minimal coverage depth are marked by quadrats. Additionally, the results of FEM-simulations are recorded by means of blue triangles.

First, the excellent consistency of the LCM-results with the FEM-results becomes obvious. For the planned coverage depth of 1.50 m we get a temperature rise of the survey point of $\Delta\Theta_P = 0.51$ K, which is considerably lower than the limit value of 2.0 K. In this case the conductor temperature reaches only 32.3°C, i.e. by far lower than the critical value of 70°C.

The minimal coverage depth of the cable, for which the limit value of 2.0 K will be reached, is 0.40 m. For this, a conductor temperature of 30.1 °C is reached.

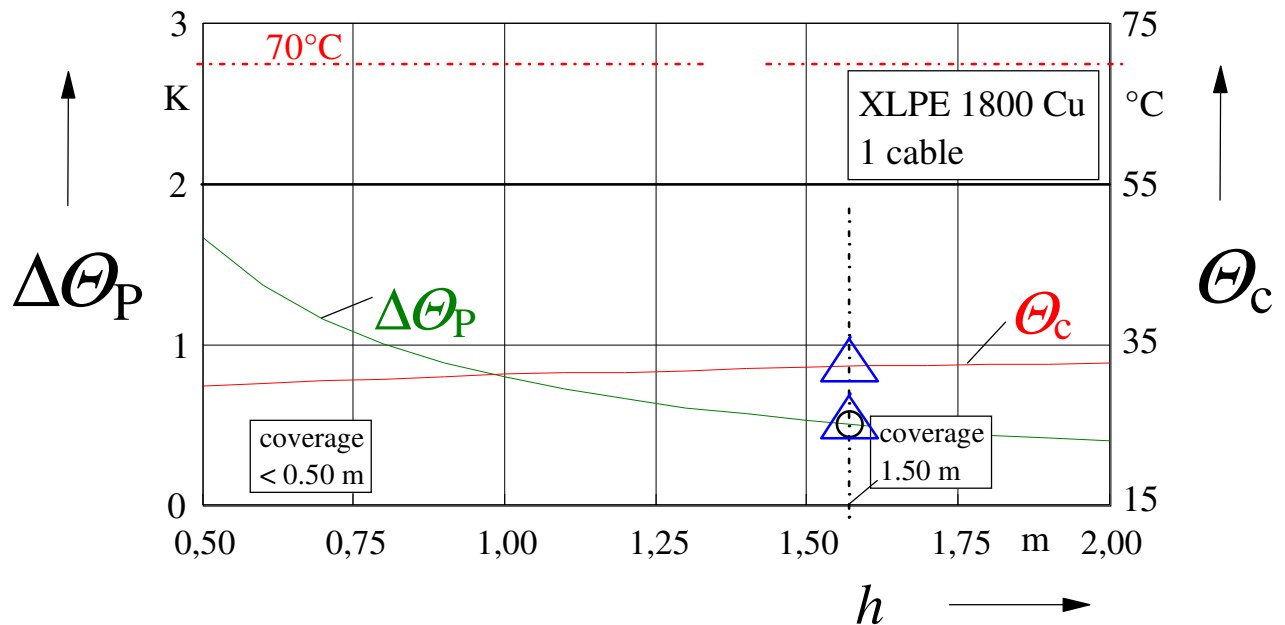


Fig. 13: Temperature rise $\Delta\Theta_P$ of survey point (green) and conductor temperature Θ_C (red) as functions of the laying depth h ; Δ = FEM-result; $\lambda = 1.43$ W/(K m); $\Theta_{\text{amb}} = 15^\circ\text{C}$, Case 1b: XLPE-cable 1800 mm² Cu-conductor, 1 cable in one trench

5.2.3 Case 2a: XLPE-cable 1600 mm² Cu-conductor, 1 cable in one trench

For this case 2a of Tab. 5 and Tab. 6 and for the given current of 1333 A each cable, in Fig. 14 the temperature rise of the survey point $\Delta\Theta_P$ (green) as well as the conductor temperature Θ_c (red) are shown as functions of the laying depth h . Again, the results for a coverage depth of 1.50 m are marked by circles, whereas those for the minimal coverage depth are marked by quadrats. Additionally, the results of FEM-simulations are recorded by means of blue triangles.

First again, the excellent consistency of the LCM-results with the FEM-results becomes obvious. For the planned coverage depth of 1.50 m we get a temperature rise of the survey point of $\Delta\Theta_P = 0.58$ K, which is considerably lower than the limit value of 2.0 K. In this case the conductor temperature reaches only 35.5 °C, i.e. by far lower than the critical value of 70 °C.

The minimal coverage depth of the cable, for which the limit value of 2.0 K will be reached, is 0.45 m. For this, a conductor temperature of 32.8 °C is reached.

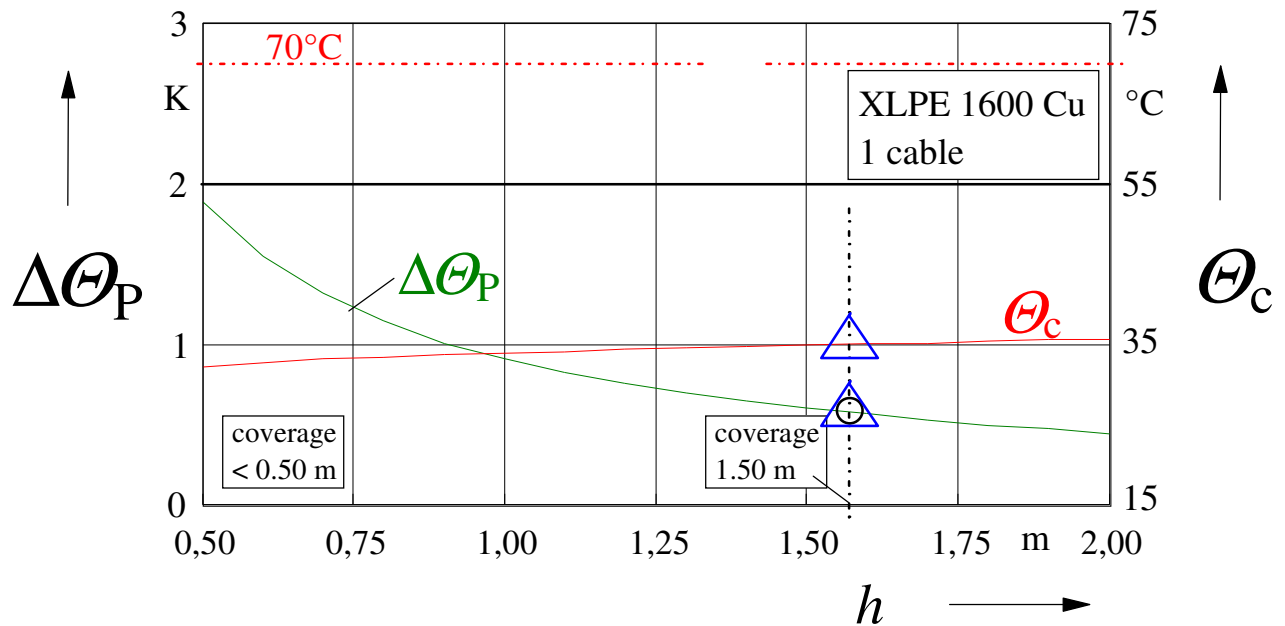


Fig. 14: Temperature rise $\Delta\Theta_P$ of survey point (green) and conductor temperature Θ_c (red) as functions of the laying depth h , Δ = FEM-result; $\lambda = 1.43$ W/(K m); $\Theta_{amb} = 15^\circ\text{C}$, case 2a: 1 XLPE-cable; $A_{Cu} = 1600$ mm²

5.2.4 Case 2b: XLPE-cable 1600 mm² Cu-conductor, 2 cables in one trench

For this case 2b of Tab. 5 and Tab. 6 and for the given current of 1333 A each cable, in Fig. 15 the temperature rise of the survey point $\Delta\Theta_P$ (green) as well as the conductor temperature Θ_c (red) are shown as functions of the laying depth h . Again, the results for a coverage depth of 1.50 m are marked by circles, whereas those for the minimal coverage depth are marked by quadrats. Additionally, the results of FEM-simulations are recorded by means of blue triangles.

First again, the excellent consistency of the LCM-results with the FEM-results becomes obvious. For the planned coverage depth of 1.50 m we get a temperature rise of the survey point of $\Delta\Theta_P = 1.19$ K, which is considerably lower than the limit value of 2.0 K. In this case the conductor temperature reaches only 42.8 °C, i.e. by far lower than the critical value of 70 °C.

The minimal coverage depth of the cable, for which the limit value of 2.0 K will be reached, is 0.86 m. For this, a conductor temperature of 40.2 °C is reached.

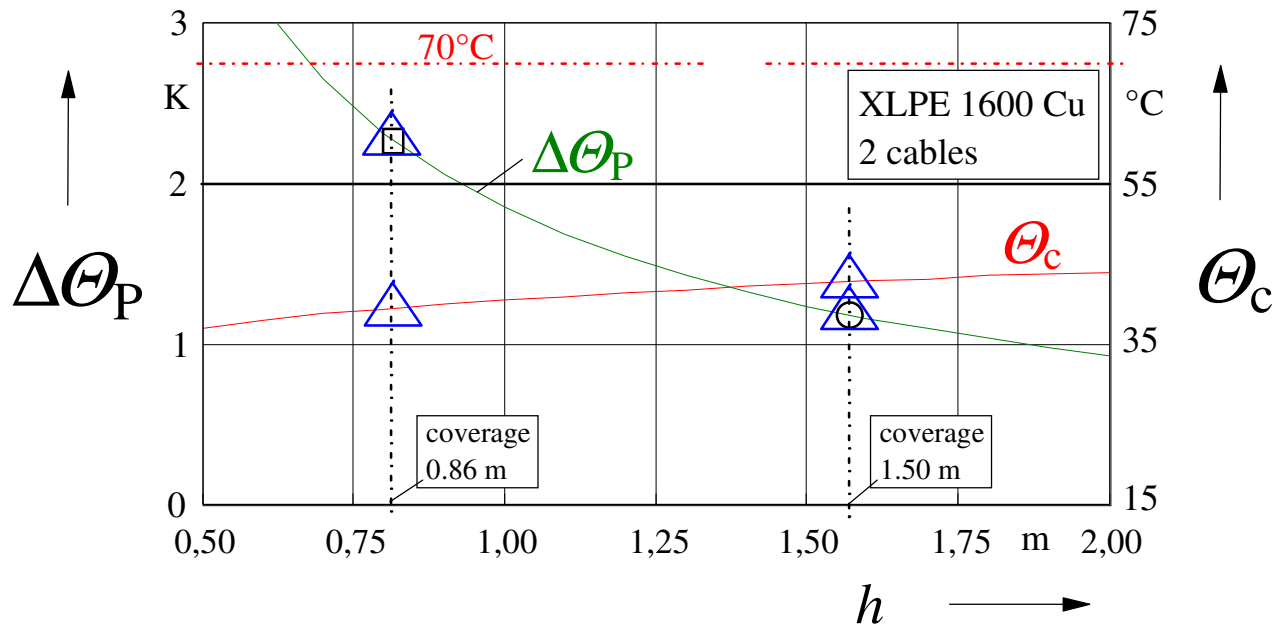


Fig. 15: Temperature rise $\Delta\Theta_P$ of survey point (green) and conductor temperature Θ_c (red) as functions of the laying depth h , Δ = FEM-result; $\lambda = 1.43$ W/(K m); $\Theta_{amb} = 15^\circ\text{C}$, case 2b: 2 XLPE-cables; $A_{Cu} = 1600$ mm²

5.2.5 Case 3a: XLPE-cable 2500 mm² Al-conductor, 2 cables in one trench

For this case 3a of Tab. 5 and Tab. 6 and for the given current of 1333 A each cable, in Fig. 16 the temperature rise of the survey point $\Delta\Theta_P$ (green) as well as the conductor temperature Θ_c (red) are shown as functions of the laying depth h . Again, the results for a coverage depth of 1.50 m are marked by circles, whereas those for the minimal coverage depth are marked by quadrats. Additionally, the results of FEM-simulations are recorded by means of blue triangles.

First again, the excellent consistency of the LCM-results with the FEM-results becomes obvious. For the planned coverage depth of 1.50 m we get a temperature rise of the survey point of $\Delta\Theta_P = 1.21\text{K}$, which is considerably lower than the limit value of 2.0 K. In this case the conductor temperature reaches only 41.7 °C, i.e. by far lower than the critical value of 70 °C.

The minimal coverage depth of the cable, for which the limit value of 2.0 K will be reached, is 0.90 m. For this, a conductor temperature of 39.1 °C is reached.

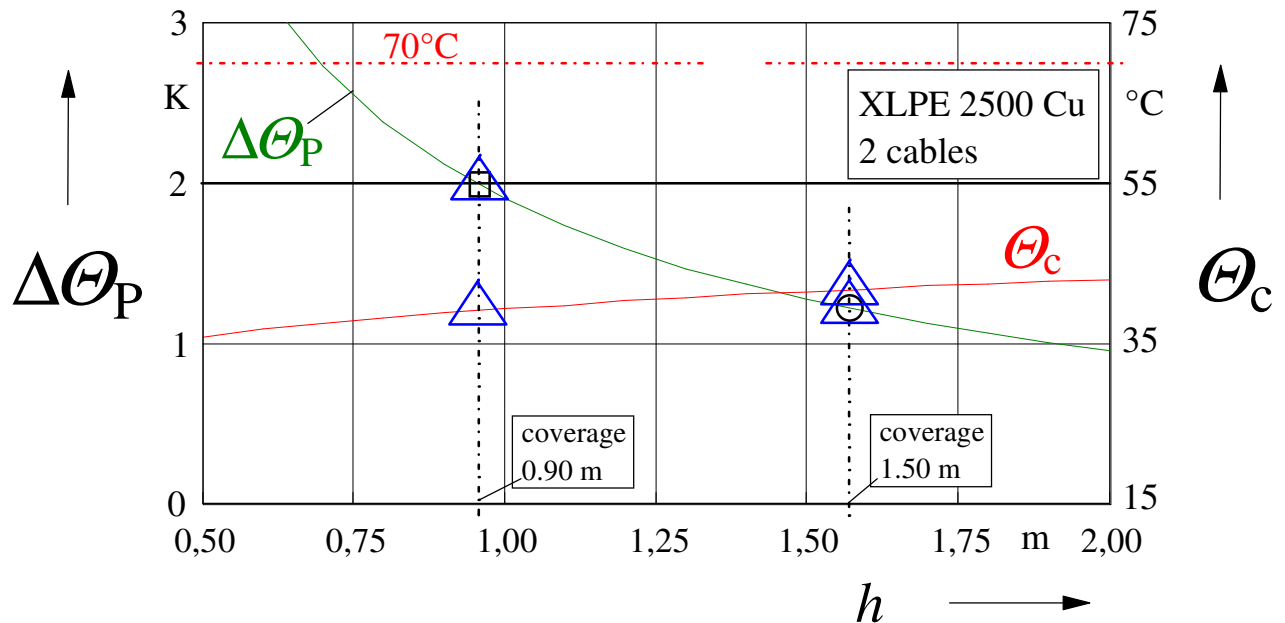


Fig. 16: Temperature rise $\Delta\Theta_P$ of survey point (green) and conductor temperature Θ_c (red) as functions of the laying depth h , Δ = FEM-result; $\lambda = 1.43 \text{ W/(K m)}$; $\Theta_{\text{amb}} = 15^\circ\text{C}$, case 3a: 2 XLPE-cable; $A_{\text{Al}} = 2500 \text{ mm}^2$

5.2.6 Case 3b: XLPE-cable 2500 mm² Al-conductor, 1 cable in one trench

For this case 3b of Tab. 5 and Tab. 6 and for the given current of 1333 A each cable, in Fig. 17 the temperature rise of the survey point $\Delta\Theta_P$ (green) as well as the conductor temperature Θ_c (red) are shown as functions of the laying depth h . Again, the results for a coverage depth of 1.50 m are marked by circles, whereas those for the minimal coverage depth are marked by quadrats. Additionally, the results of FEM-simulations are recorded by means of blue triangles.

First again, the excellent consistency of the LCM-results with the FEM-results becomes obvious. For the planned coverage depth of 1.50 m we get a temperature rise of the survey point of $\Delta\Theta_P = 0.59$ K, which is considerably lower than the limit value of 2.0 K. In this case the conductor temperature reaches only 34.0 °C, i.e. by far lower than the critical value of 70 °C.

The minimal coverage depth of the cable, for which the limit value of 2.0 K will be reached, is 0.45 m. For this, a conductor temperature of 31.6°C is reached.

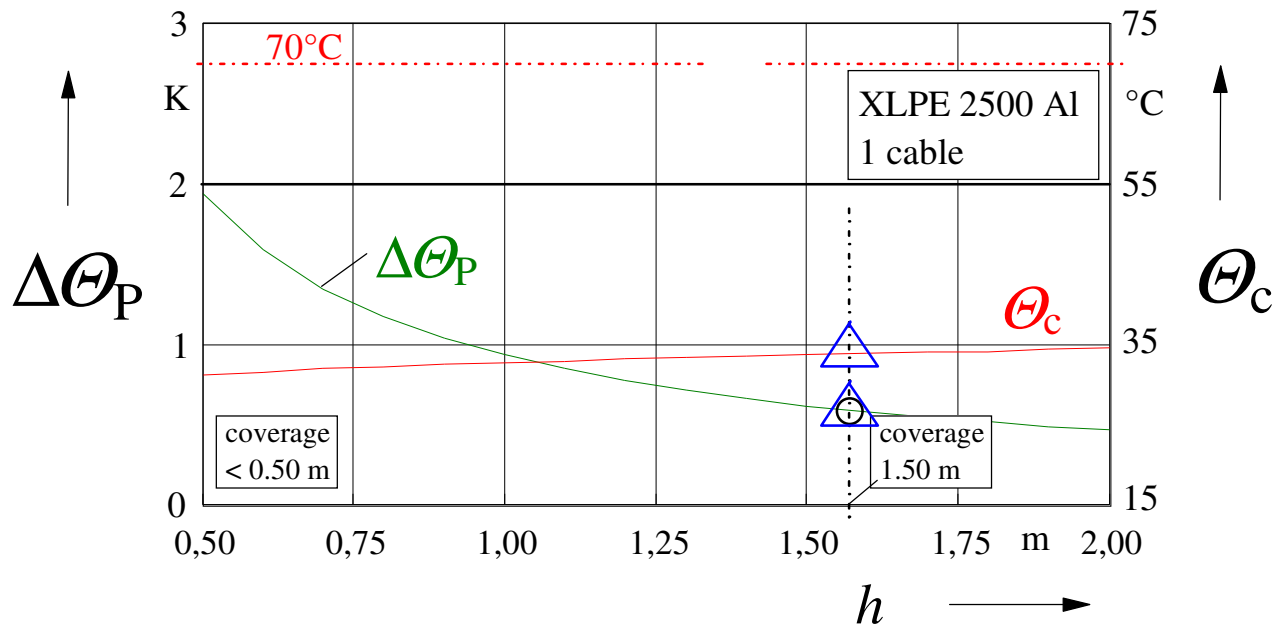


Fig. 17: Temperature rise $\Delta\Theta_P$ of survey point (green) and conductor temperature Θ_c (red) as functions of the laying depth h , Δ = FEM-result; $\lambda = 1.43$ W/(K m); $\Theta_{amb} = 15^\circ\text{C}$, case 3b: 1 XLPE-cable; $A_{Al} = 2500$ mm²

5.2.7 Case 4a: XLPE-cable 2000 mm² Al-conductor, 1 cable in one trench

For this case 4a of Tab. 5 and Tab. 6 and for the given current of 1333 A each cable, in Fig. 18 the temperature rise of the survey point $\Delta\Theta_P$ (green) as well as the conductor temperature Θ_c (red) are shown as functions of the laying depth h . Again, the results for a coverage depth of 1.50 m are marked by circles, whereas those for the minimal coverage depth are marked by quadrats. Additionally, the results of FEM-simulations are recorded by means of blue triangles.

First again, the excellent consistency of the LCM-results with the FEM-results becomes obvious. For the planned coverage depth of 1.50 m we get a temperature rise of the survey point of $\Delta\Theta_P = 0.76$ K, which is considerably lower than the limit value of 2.0 K. In this case the conductor temperature reaches only 40.8 °C, i.e. by far lower than the critical value of 70 °C.

The minimal coverage depth of the cable, for which the limit value of 2.0 K will be reached, is 0.55 m. For this, a conductor temperature of 37.8 °C is reached.

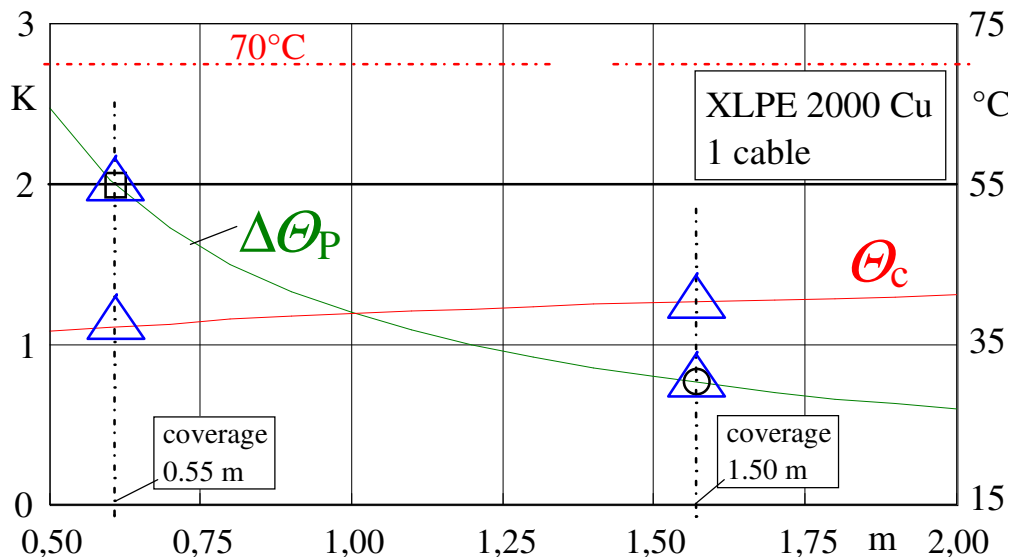


Fig. 18: Temperature rise $\Delta\Theta_P$ of survey point (green) and conductor temperature Θ_c (red) as functions of the laying depth h , Δ = FEM-result; $\lambda = 1.43$ W/(K m); $\Theta_{amb} = 15^\circ\text{C}$, case 4a: 1 XLPE-cable; $A_{Al} = 2000$ mm²

5.2.8 Case 4b: XLPE-cable 2000 mm² Al-conductor, 2 cables in one trench

For this case 4b of Tab. 5 and Tab. 6 and for the given current of 1333 A each cable, in Fig. 19 the temperature rise of the survey point $\Delta\Theta_P$ (green) as well as the conductor temperature Θ_c (red) are shown as functions of the laying depth h . Again, the results for a coverage depth of 1.50 m are marked by circles, whereas those for the minimal coverage depth are marked by quadrats. Additionally, the results of FEM-simulations are recorded by means of blue triangles.

First again, the excellent consistency of the LCM-results with the FEM-results becomes obvious. For the planned coverage depth of 1.50 m we get a temperature rise of the survey point of $\Delta\Theta_P = 1.58$ K, which is considerably lower than the limit value of 2.0 K. In this case the conductor temperature reaches only 50.8 °C, i.e. by far lower than the critical value of 70 °C.

The minimal coverage depth of the cable, for which the limit value of 2.0 K will be reached, is 1.16 m. For this, a conductor temperature of 49.1 °C is reached.

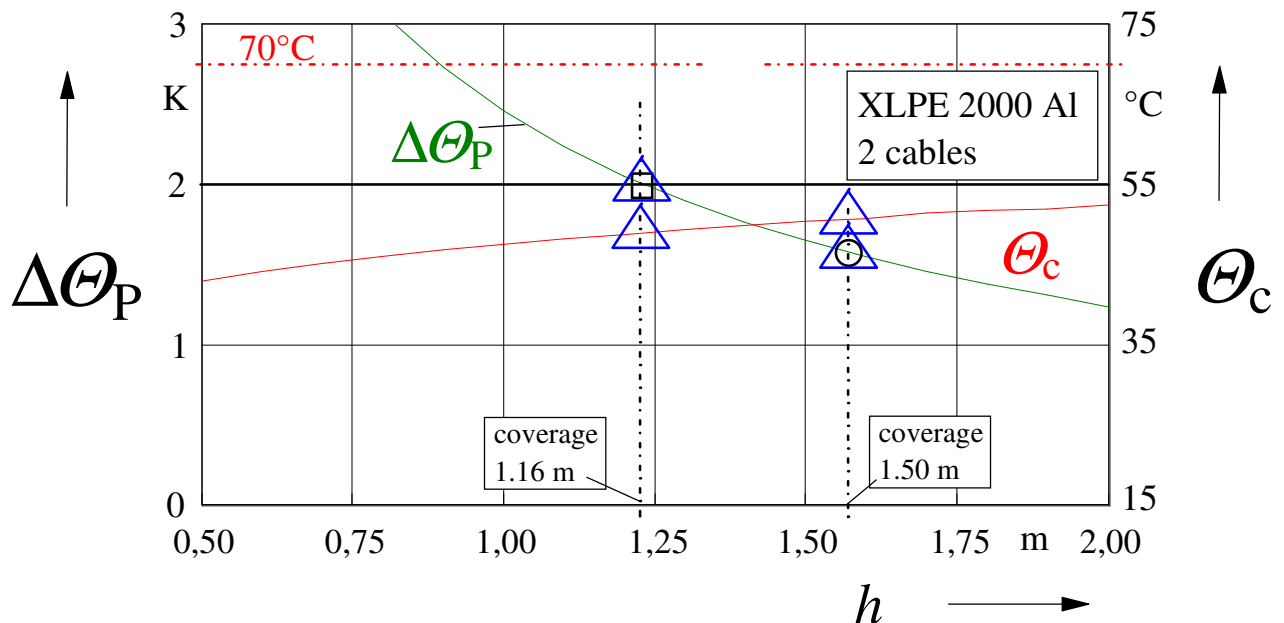


Fig. 19: Temperature rise $\Delta\Theta_P$ of survey point (green) and conductor temperature Θ_c (red) as functions of the laying depth h , Δ = FEM-result; $\lambda = 1.43$ W/(K m); $\Theta_{amb} = 15^\circ\text{C}$, case 4b: 2 XLPE-cables; $A_{Al} = 2000$ mm²

5.2.9 Case 5a: MIND-cable 2000 mm² Cu-conductor, 2 cables in one trench

For this case 5a of Tab. 5 and Tab. 6 and for the given current of 1333 A each cable, in Fig. 20 the temperature rise of the survey point $\Delta\Theta_P$ (green) as well as the conductor temperature Θ_c (red) are shown as functions of the laying depth h . Again, the results for a coverage depth of 1.50 m are marked by circles, whereas those for the minimal coverage depth are marked by quadrats. Additionally, the results of FEM-simulations are recorded by means of blue triangles.

First again, the excellent consistency of the LCM-results with the FEM-results becomes obvious. For the planned coverage depth of 1.50 m we get a temperature rise of the survey point of $\Delta\Theta_P = 0,94$ K, which is considerably lower than the limit value of 2.0 K. In this case the conductor temperature reaches only 40.9 °C, i.e. by far lower than the critical value of 55 °C.

The minimal coverage depth of the cable, for which the limit value of 2.0 K will be reached, is 0.70 m. For this, a conductor temperature of 37.1 °C is reached.

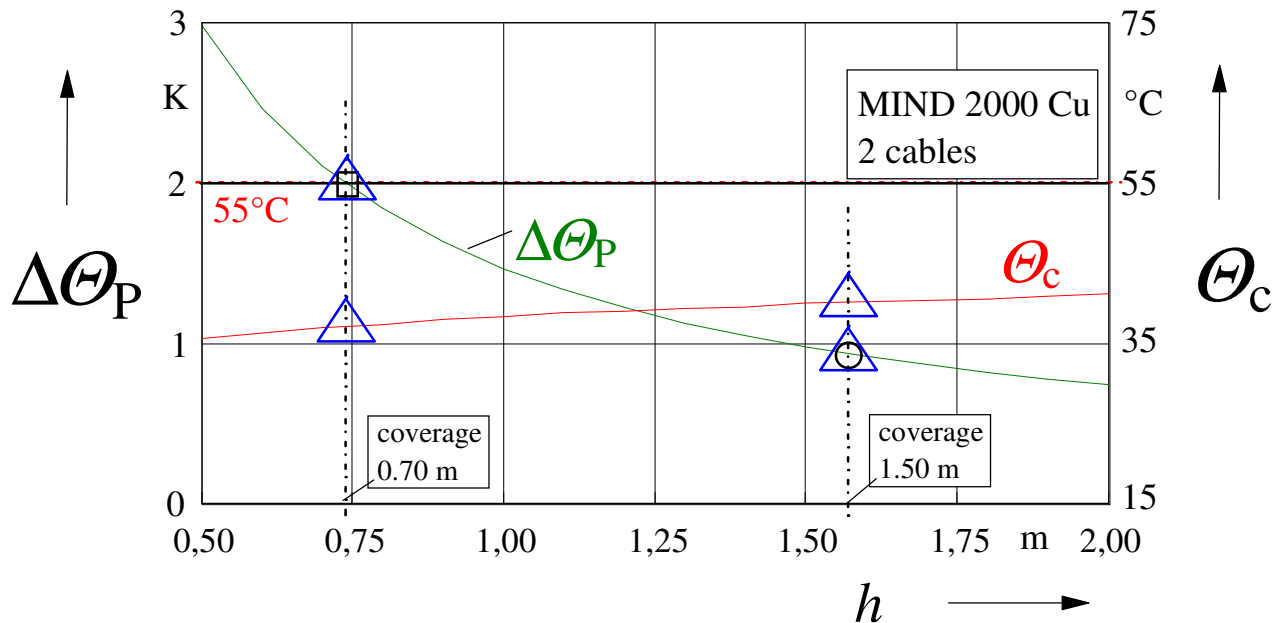


Fig. 20: Temperature rise $\Delta\Theta_P$ of survey point (green) and conductor temperature Θ_c (red) as functions of the laying depth h , Δ = FEM-result; $\lambda = 1.0$ W/(K m); $\Theta_{amb} = 15^\circ\text{C}$, case 5a: 2 MIND-cables; $A_{Cu} = 2000$ mm²

5.2.10 Case 5b: MIND-cable 2000 mm² Cu-conductor, 1 cable in one trench

For this case 5b of Tab. 5 and Tab. 6 and for the given current of 1333 A each cable, in Fig. 21 the temperature rise of the survey point $\Delta\Theta_P$ (green) as well as the conductor temperature Θ_c (red) are shown as functions of the laying depth h . Again, the results for a coverage depth of 1.50 m are marked by circles, whereas those for the minimal coverage depth are marked by quadrats. Additionally, the results of FEM-simulations are recorded by means of blue triangles.

First again, the excellent consistency of the LCM-results with the FEM-results becomes obvious. For the planned coverage depth of 1.50 m we get a temperature rise of the survey point of $\Delta\Theta_P = 0.46$ K, which is considerably lower than the limit value of 2.0 K. In this case the conductor temperature reaches only 33.9 °C, i.e. by far lower than the critical value of 55 °C.

The minimal coverage depth of the cable, for which the limit value of 2.0 K will be reached, is 0.35 m. For this, a conductor temperature of 32.4°C is reached.

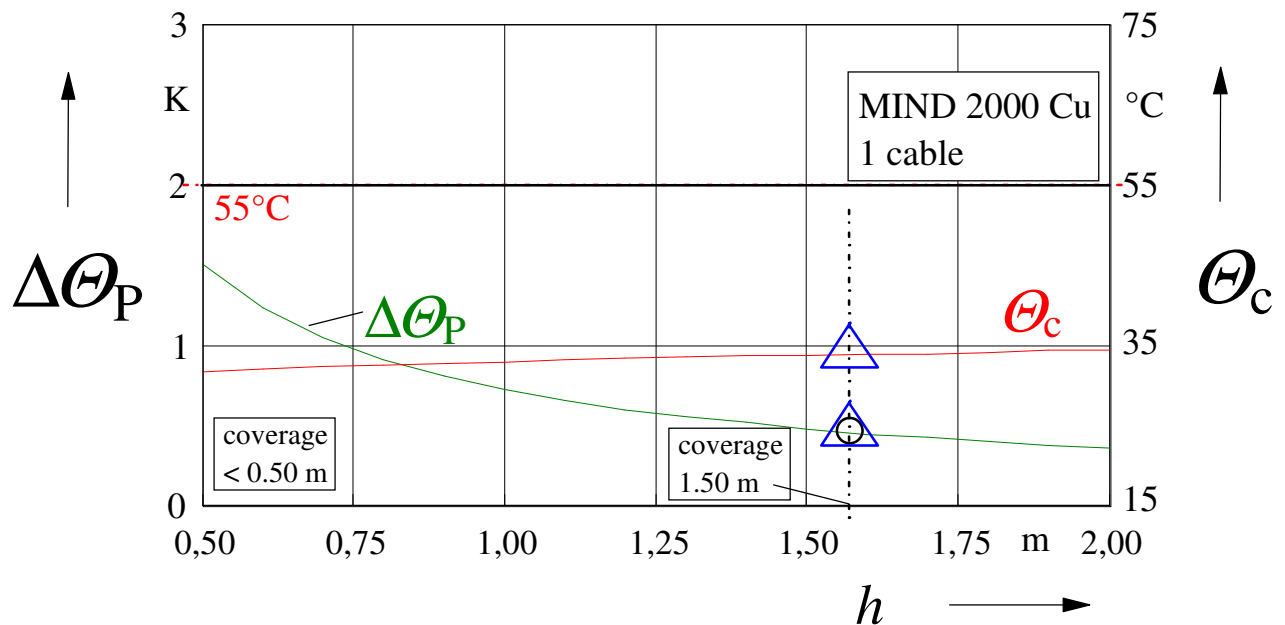


Fig. 21: Temperature rise $\Delta\Theta_P$ of survey point (green) and conductor temperature Θ_c (red) as functions of the laying depth h , Δ = FEM-result; $\lambda = 1.0$ W/(K m); $\Theta_{amb} = 15^\circ\text{C}$, case 5b: 1 MIND-cable; $A_{Cu} = 2000$ mm²

5.2.11 Case 6a: MIND-cable 1800 mm² Cu-conductor, 1 cable in one trench

For this case 6a of Tab. 5 and Tab. 6 and for the given current of 1333 A each cable, in Fig. 22 the temperature rise of the survey point $\Delta\Theta_P$ (green) as well as the conductor temperature Θ_c (red) are shown as functions of the laying depth h . Again, the results for a coverage depth of 1.50 m are marked by circles, whereas those for the minimal coverage depth are marked by quadrats. Additionally, the results of FEM-simulations are recorded by means of blue triangles.

First again, the excellent consistency of the LCM-results with the FEM-results becomes obvious. For the planned coverage depth of 1.50 m we get a temperature rise of the survey point of $\Delta\Theta_P = 0.52$ K, which is considerably lower than the limit value of 2.0 K. In this case the conductor temperature reaches only 37.4 °C, i.e. by far lower than the critical value of 55 °C.

The minimal coverage depth of the cable, for which the limit value of 2.0 K will be reached, is 0.40 m. For this, a conductor temperature of 34.8 °C is reached.

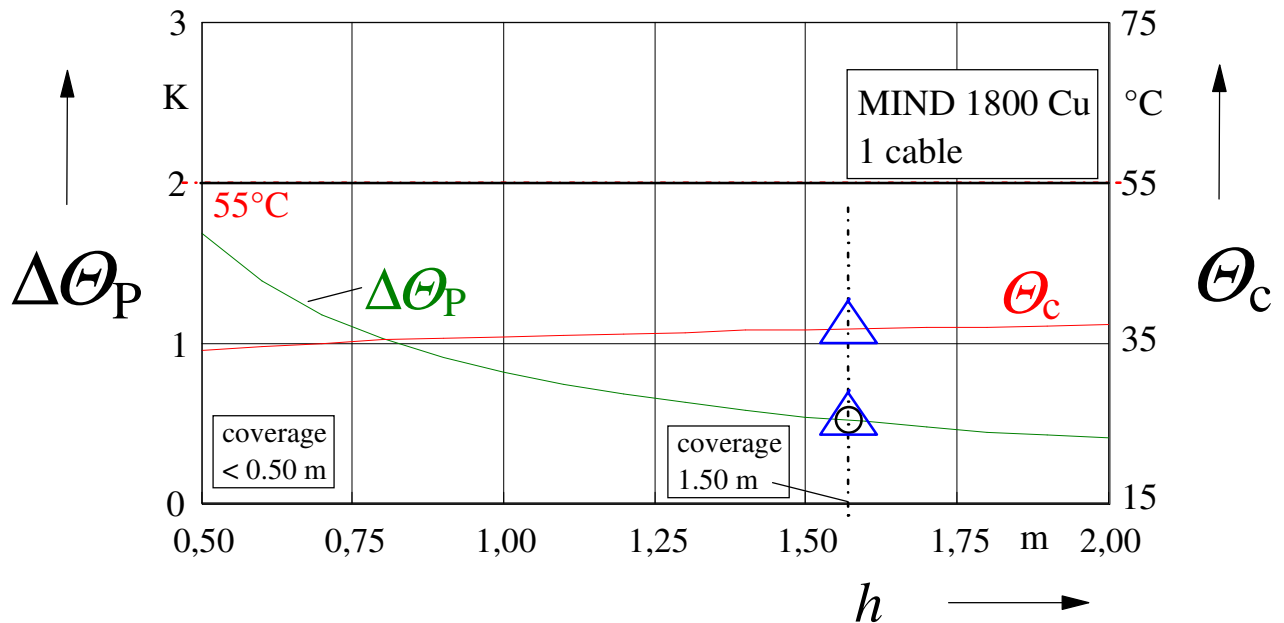


Fig. 22: Temperature rise $\Delta\Theta_P$ of survey point (green) and conductor temperature Θ_c (red) as functions of the laying depth h , Δ = FEM-result; $\lambda = 1.0$ W/(K m); $\Theta_{amb} = 15^\circ\text{C}$, case 6a: 1 MIND-cable; $A_{Cu} = 1800$ mm²

5.2.12 Case 6b: MIND-cable 1800 mm² Cu-conductor, 2 cables in one trench

For this case 6b of Tab. 5 and Tab. 6 and for the given current of 1333 A each cable, in Fig. 23 the temperature rise of the survey point $\Delta\Theta_P$ (green) as well as the conductor temperature Θ_c (red) are shown as functions of the laying depth h . Again, the results for a coverage depth of 1.50 m are marked by circles, whereas those for the minimal coverage depth are marked by quadrats. Additionally, the results of FEM-simulations are recorded by means of blue triangles.

First again, the excellent consistency of the LCM-results with the FEM-results becomes obvious. For the planned coverage depth of 1.50 m we get a temperature rise of the survey point of $\Delta\Theta_P = 1.06$ K, which is considerably lower than the limit value of 2.0 K. In this case the conductor temperature reaches only 43.9 °C, i.e. by far lower than the critical value of 55 °C.

The minimal coverage depth of the cable, for which the limit value of 2.0 K will be reached, is 0.77 m. For this, a conductor temperature of 41.0 °C is reached.

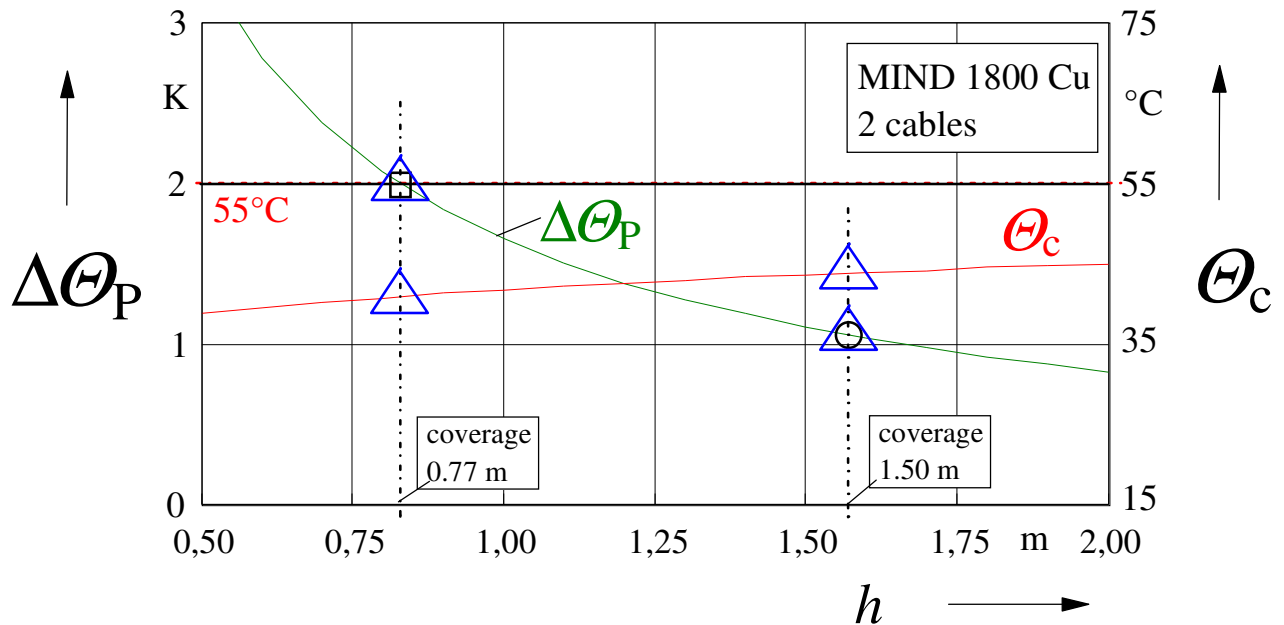


Fig. 23: Temperature rise $\Delta\Theta_P$ of survey point (green) and conductor temperature Θ_c (red) as functions of the laying depth h , Δ = FEM-result; $\lambda = 1.0$ W/(K m); $\Theta_{amb} = 15^\circ\text{C}$, case 6b: 2 MIND-cables; $A_{Cu} = 1800$ mm²

6 Summary

National Grid Viking Link Limited (NGVL) and Energinet.dk are projecting a new High Voltage Direct-Current (HVDC) submarine transmission line between Great Britain and Denmark, known as Viking Link, which will be connected with the existing Danish and British onshore transmission systems. Viking Link will be operated with a nominal voltage of 525 kV and with a maximum load of 1.400-MW (2x1333 A).

The offshore-part of the route consists of two single-core submarine cables, which are laid into the seabed and which will transmit direct current over a length of 630 km between the coasts of Great Britain and Denmark. The offshore cable route is crossing the exclusive economic zones (AWZ) of Great Britain, The Netherlands, Germany and Denmark.

In the frame of the approval procedure and for submission at the BSH (“Bundesamt für Seeschifffahrt und Hydrographie”, respectively “Federal Maritime and Hydrographic Agency”), in this study the question has been examined, if the 2 K-criterion, which is given in the German AWZ, can be satisfied with the hitherto designed cable constructions and laying depths. Six different cables, predetermined by the client, with two laying arrangements each, have been examined.

In a third step extensive investigations by means of the LCM method were made to compare with the FEM results and to show the dependency of the temperature rise at the survey point as well as the cable temperatures on the laying depth.

A summary of the results with the temperature rises of the survey point and the cable temperatures (temperatures of conductor and cable surface) for a coverage depth of 1.50 m is given in table 7. Additionally, the minimal coverage depths and the corresponding cable temperatures are listed.

In all cases, the cables cause temperature rises in the seabed at a depth of 0.2 m, which are far smaller than 2 K. In a second step the minimum necessary coverage depths for all twelve cases have been determined with the result, that none of the six cables, even in the bundled arrangement, requires a covering depth of 1.50 m meters.

Table 7 elucidates, that for a coverage depth of 1.50 m quite essential reserves are given with respect to the 2-K-criterion. This means, that – depending on the considered case – by far smaller coverage depths than 1.5 m are possible.

It should be mentioned that all considerations were done by far on the safe side: this applies to the thermal resistivity of the seabed with $\rho = 0.7 \text{ K m/W}$ and furthermore to the chosen undisturbed temperature of the seabed of 15°C . Even more important is the fact, that all analysis has been done on the base of a continuous load, i.e. for a current, that will be constant over all the operating time. This appears to be somewhat unrealistic: experience shows, that the transmission load in such systems will by no means be constant, but that it will undergo daily, weekly and seasonal variations. Otherwise, the cable and its surrounding are presenting an extremely inert thermal system (reaching a stationary conductor temperature after a load step needs more than one year!), so that the consideration of an only slightly reduced daily load factor (i.e. mean value of current, related to its peak value) of e.g. $m = 0.85 \dots 0.90$ would enable further, sensible temperature reductions of the cable and its surrounding or, alternatively, further reductions of the laying depth.

HVDC cable 525 kV		$\Delta\Theta_{P,1.5m}$	$\Theta_{c,1.5m}$	$\Theta_{S,1.5m}$	$h_{c,min}$	$\Theta_{c,min}$	$\Theta_{S,min}$
case	cable	K	°C	°C	m	°C	°C
1a	XLPE 1800 Cu 2 cables	1.03	39.0	28.3	0.75	36.2	25.5
1b	XLPE 1800 Cu 1 cable	0.51	32.6	22.3	0.40	30.1	19.8
2a	XLPE 1600 Cu 1 cable	0.58	35.5	23.4	0.45	32.8	20.7
2b	XLPE 1600 Cu 2 cables	1.18	43.0	30.2	0.85	40.3	27.7
3a	XLPE 2500 Al 2 cables	1.21	41.7	30.3	0.90	39.3	27.9
3b	XLPE 2500 Al 1 cable	0.59	34.3	23.4	0.45	31.6	20.7
4a	XLPE 2000 Al 1 cable	0.76	40.8	25.9	0.55	37.8	23.0
4b	XLPE 2000 Al 2 cables	1.57	50.9	35.0	1.15	49.1	33.3
5a	MIND 2000 Cu 2 cables	0.94	40.9	27.1	0.70	38.0	24.3
5b	MIND 2000 Cu 1 cable	0.46	34.9	21.7	0.35	32.4	19.2
6a	MIND 1800 Cu 1 cable	0.52	37.4	22.5	0.40	34.8	20.0
6b	MIND 1800 Cu 2 cables	1.06	44.3	28.8	0.75	41.4	26.9

Tab. 7: summary of the results with temperature rises of survey point and conductor temperatures for a coverage depth of 1.50 m as well as for the minimal coverage depths with corresponding conductor and surface temperatures; thermal conductivity of seabed: $\lambda = 1.43 \text{ W/(K m)}$

Legend:

$\Delta\Theta_{P,1.5m}$	temperature rise of survey point for coverage depth of 1.5 m
$\Theta_{c,1.5m}$	conductor temperature for coverage depth of 1.5 m
$\Theta_{S,1.5m}$	surface temperature for coverage depth of 1.5 m
$h_{c,min}$	minimal coverage depth for the 2 K-limit
$\Theta_{c,min}$	conductor temperature for minimal coverage depth
$\Theta_{S,min}$	surface temperature for minimal coverage depth

7 Annex

7.1 References

- [Bar1977] C.C. Barnes: Submarine telecommunication and power cables, P. Peregrinus LTD., Stevenage, 1977
- [BMU2011] BMU: „Ökologische Auswirkungen von 380-kV-Erdleitungen und HGÜ-Erdleitungen“, Federal Ministry for the Environment, Nature Conservation, Buildings and Nuclear Safety, FKZ 03MAP189, Berlin 2011
- [Bra2004] H. Brakelmann: „Kabelverbindung der Offshore-Windfarm GlobalTech I zum Netzanschluss- Punkt“, technical study, Rheinberg, 2004
- [Bra2010] H. Brakelmann: „Kabelverbindung der Offshore-Windfarm Riffgat zum Festland“, study for Transpower Offshore GmbH, Bayreuth
- [BS2006] H. Brakelmann, J. Stammen: “Thermal analysis of Submarine Cable routes: LSM or FEM?”, IEEE-conf. PECon (2006) , Putra Jaya, pp. 560 - 565
- [BSH2007] BSH: Konstruktive Ausführung von Offshore-Windenergieanlagen“, German Maritime and Hydrographic Agency (BSH), June 2007
- [Eve2016] G. Evenset e.a.: ”Thermal characterization of seabed along the NordLink cable route – results and comparison of measurement methods”, Cigré-report B1-313, CIGRE-Conf. 2016, Paris
- [Fri2010] Fricke: „Erwärmungsberechnungen für Kabelanlagen zur Anbindung von Offshore-Windparks im Bereich Norderney“, Technical study, Siemens, 2008
- [FUG2016] FUGRO: „VIKING LINK CABLE ROUTE SURVEY“, National Grid Interconnector Holdings Limited, 2016
- [GWS2014] Generaldirektion Wasserstraßen und Schifffahrt: Richtlinie „Offshore-Anlagen“, zur Gewährleistung der Sicherheit und Leichtigkeit des Schiffverkehrs, Version 2.0“, www.ast-nordwest.gdws.wsv.de/schifffahrt/Windparks_auf_hoher_See/PDF/20140701_WSV_RiLi_Offshore_Anlagen_FINAL.pdf
- [IEC2006] International Electrotechnical Commission: “Electric cables – Calculation of the current rating Part 1-1:Current rating equation (100 % load factor) and calculation of losses”, General IEC-Publ. 60287-1-1, Paris, second edition, 2006-12
- [Nat2016] Nationalgrid, ENERGINET/DK: „Viking Link Verbindungsleitung, Verbindung der dänischen und britischen Strom-Versorgungssysteme“ Informationsbroschüre zur Öffentlichkeitsbeteiligung im Rahmen der TEN-E-Verordnung
- [RB2004] F. Richert, H. Brakelmann: „Bemessung der Energiekabel zur Netzanbindung on Offshore- Windfarmen“, El.wirtsch. 103 (2004), pp. 56-59
- [Smo2001] Smolczyk, U.: Grundbau Taschenbuch Teil2, Geotechnische Verfahren, Kap. 2.4, Tab. 3: Anhaltswerte zur Wärmeleitfähigkeit wassergesättigter Böden, Ernst&Sohn-Verlag, Berlin, 6. Aufl. (24. April 2001)
- [Sta2001] J. Stammen, „Numerische Berechnung elektromagnetischer und thermischer Felder in Hochspannungskabelanlagen“, Dissertation Universität Duisburg, Shaker Verlag, 2001
- [Rei2012] <http://www.reise-klima.de/klima/41-Sylt>

7.2 Publication: Current rating analysis for cable installations with temperature restrictions

H. Brakelmann (published – in German – in ew 12/2016)

0. Problem

The installation of submarine cables in the German North Sea or in the Baltic Sea is subjected to a temperature restriction, the 2 K-criterion [1]. This means, that a so-called “ecological point” in the seabed, situated in a depth h_P directly above the cable (see fig.1, left), is not permitted to heat by more than 2.0 K by the cable losses. Normally, the depth of this point is defined to $h_P = 0.2$ m, except for the national park “Niedersächsisches Wattenmeer”, where it is $h_P = 0.3$ m. In praxi, the 2 K-criterion may have tremendous effects on the cable design, - in much cases enforcing greater laying depths in the sea ground and/or more expensive cables with enlarged conductor cross-sections.

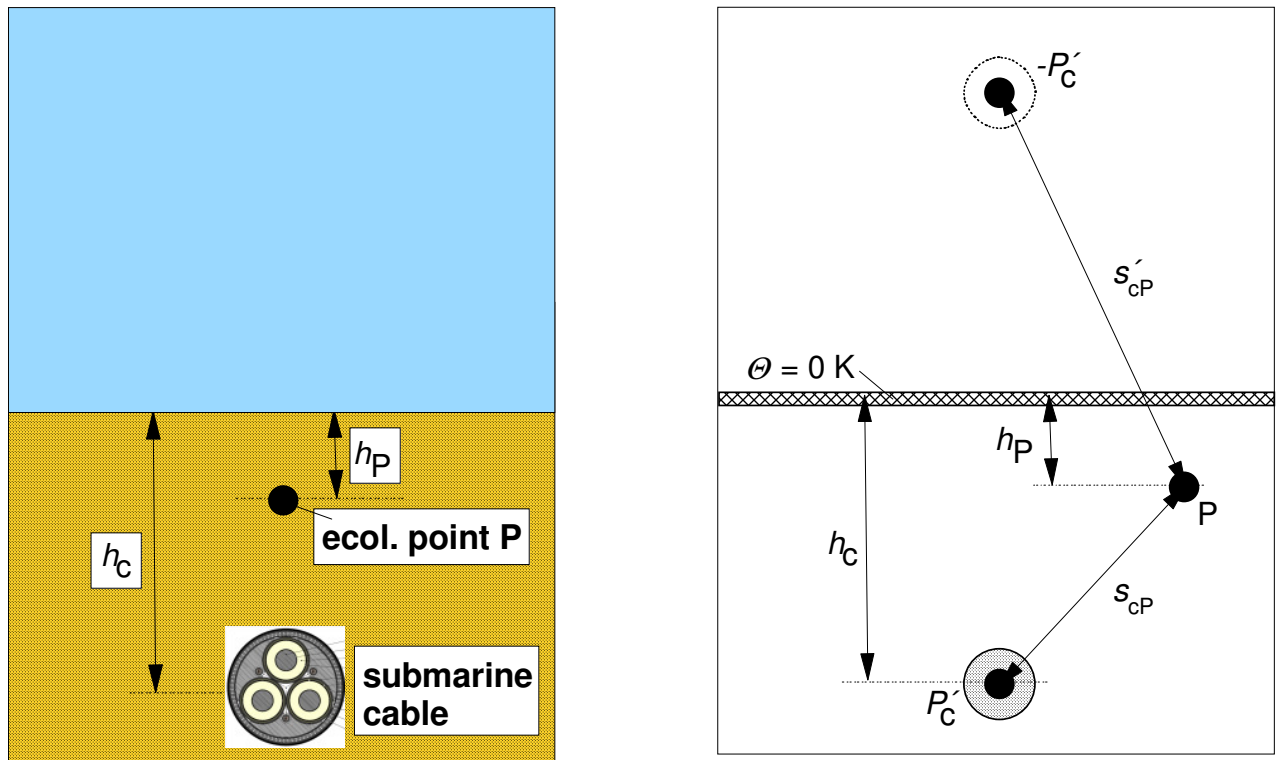


fig. 1: 2 K-criterion for the survey point P above the submarine cable with the power losses P_C' , right: representation of the sea bottom as a thermal sink by means of a mirrored thermal source with the power losses $(-P_C')$

In a study of the Federal Ministry for the Environment, Nature Conservation, Buildings and Nuclear Safety „Ecological impact of 380-kV-cables and HVDC cables“ [2] a prevention value of the maximum temperature rise in the soil because of high voltage cables is requested: „Such a value could be approximately 5 K in a depth of 50 cm below soil surface.“[2]. That means that for onshore cable routes, too, in the future such restrictions of soil heating by cables are imaginable. Further possible examples are temperature restrictions in the case of adjacent infrastructural lines, as e.g. pipes for gas, water etc.

In such situations, the design of the cables must be orientated both at the highest permissible temperature inside the cable (conductor temperature) as well as at the highest permissible

temperature of a certain point in the trench, i.e. two current ratings of the cable are to be identified.

As far as export cables of offshore windfarms are concerned, temperature rises and current ratings should by no means be calculated for constant transmission power (continuous rating): typically, a critical yearly load cycle is derived from measured wind velocities, and from this load cycle a time-restricted peak load phase as well as a preload phase are derived [3]. As an example the specification of one TSO for the 2 K-criterion is a seven-day full load period, combined with two foregoing and following 45-day periods with 77 % of the full load. By means of this scenario, the 2 K-criterion should be satisfied even for the worst winter conditions. The implementation of this request is shown in fig. 2 for the initial phases of the two loss cycles 1 and 2.

Calculations of the transient temperature rises and of the resulting current ratings, based on such yearly load cycles, are complex. For simplification, in the following some rating equations will be derived, which on the one hand take the complex dynamic processes into account but which on the other hand can be handled in a similar simple manner as with the rating equation of IEC-publication 60287 for continuous load [4].

1. Temperature rise of the survey point caused by a step of the cable losses

The stationary thermal coupling between a cable and other cables or other survey points are mostly calculated by means of the Kenelly formulae, thus following the IEC-standard 60287 [4]. This formula is based on the arrangement in fig. 1 (right) of two line sources, - one in the cable axis and the other mirrored at the soil surface, thus enforcing the soil surface as isotherm with a temperature rise of $\Delta\Theta = 0$ K. The same arrangement can be taken as a basis for the consideration of a step of the cable losses.

If the cable's power losses make a step $\Delta P_i'$ at the time $t = 0$ in a homogeneous medium, the representing line source causes a cylindrical thermal wave, which can be described analytically as a function of space and time by means of equ. (1). The temperature rise in a distance r from the line source is

$$\Delta\theta(t) = \Delta P' \cdot \frac{1}{4 \cdot \pi \cdot \lambda} \cdot \text{E1} \left[\frac{r^2}{4 \cdot \delta \cdot t} \right] \quad (1)$$

Where E1 is the exponential-integral-function

$$\text{E1}(z) = \int_z^{\infty} \frac{e^{-u}}{u} \cdot du \quad . \quad (2)$$

or in form of a series expansion

$$\text{E1}(x) = -0,5772 - \ln x - \sum_{n=1}^{\infty} (-1)^n \cdot \frac{x^n}{(n \cdot n!)} \quad . \quad (3)$$

This exponential-integral-function is well known and given in tables as well as in terms of approximation functions [5], [6], which can easily be transferred into a simple computation program (e.g. [7]).

Taking the distances, as defined in fig. 1), of the line source and of the mirrored line source to the survey point into regard, the time-dependent temperature rise results to

$$\Delta\theta_p(t) = \Delta P' \cdot \frac{1}{4 \cdot \pi \cdot \lambda} \cdot \left\{ \text{Ei} \left[\frac{s_{\text{CP}}^2}{4 \cdot \delta \cdot t} \right] - \text{Ei} \left[\frac{s_{\text{CP}}'^2}{4 \cdot \delta \cdot t} \right] \right\} \quad (4)$$

The thermal diffusion coefficient δ can be estimated, following IEC-publ. 60853 [5], as a function of the thermal conductivity λ of the soil:

$$\delta = \left[\frac{\lambda}{\text{W}/(\text{K m})} \right]^{0.8} \cdot 4.68 \cdot 10^{-7} \frac{\text{m}^2}{\text{s}} \quad (5)$$

Equation (4) describes the thermal behavior of a survey point under the approximation, that the thermal parameters inside the cable are the same as those in the soil, i.e. it holds true for small cable diameters. Since the thermal capacitances inside the cable are greater than those of the soil, the calculation is on the safe side. Actually, the initial phase of the course of the temperature rise will be somewhat delayed, which in the corresponding IEC-standard 60 253 [5] is considered by means of an attainment factor $\alpha(t)$, which indeed can be set to 1.0 for the here considered time periods of several days.

2. Temperature rise of the survey point for a load cycle

Let cycle 2 in fig. 2 be given as a yearly cycle of the cable losses, which is characterized by a seven-day full load period of current (100 %) and losses (100 %), combined with two foregoing and following 45-day periods with 77 % of the full load current and of 59.3 % of the full load losses, respectively. This corresponds to the request of the TSO with respect to the 2 K-criterion. In the cycle 2 of fig. 2 two further levels of load or losses, respectively, are considered (rel. currents of 65.0 % and of 25.0 %), which lead to a realistic cutoff of the yearly mean value of the load current by 55.0 %.

The peak value \hat{P}'_c of the conductor losses, which appears for the peak value of the conductor temperature $\hat{\theta}_c$ during the cycle, can be expressed as

$$\hat{P}'_c = R'_c(\hat{\theta}_c) \cdot I_p^2 = \frac{\Delta\theta_{\text{P,max}} - \Delta\theta_{\text{d,P}}}{n \cdot (1 + \lambda_1 + \lambda_2) \cdot T'_{\text{trans,P}}} \quad (6)$$

The variables of equ. (6) are explained in table 1, where their numerical values are given for a concrete example.

The thermal coupling resistance $T'_{\text{Trans,P}}$ between survey point P and cable is calculated for the given time course of the cable losses $P'(t)$ with the loss steps $\Delta P'_i$ at the times t_i by scanning the time course of the resulting temperature rise with small time steps (e.g. of 1 h) and by searching the maximum temperature rise of the survey point:

$$T'_{\text{trans,P}} = \frac{1}{\hat{P}'_c} \cdot \text{Max} \left\{ \sum_{i=1}^{n_{\text{step}}} \Delta P'_i \cdot \text{SFR} \right\} \quad (7a)$$

With the peak value of the cable losses \hat{P}' (100 %) and with SFR the thermal step response (step function reaction)

$$\text{SFR} = \frac{1}{4 \cdot \pi \cdot \lambda} \cdot \sum_{i=1}^{n_{\text{step}}} \left[\text{E1}\left(\frac{s_{\text{CP}}^2}{4 \cdot \delta \cdot (t_x - t_i)}\right) - \text{E1}\left(\frac{s'_{\text{CP}}{}^2}{4 \cdot \delta \cdot (t_x - t_i)}\right) \right] \quad (7b)$$

where t_x point of time, which is varied in short periods of the time course (e.g. h) to find the maximum
 n_{step} number of power loss steps $\Delta P_i'$ at the time t_i with $t_i < t_x$,
 s_{CP} distance between cable axis and survey point and
 s'_{CP} distance between the mirrored cable and the survey point.

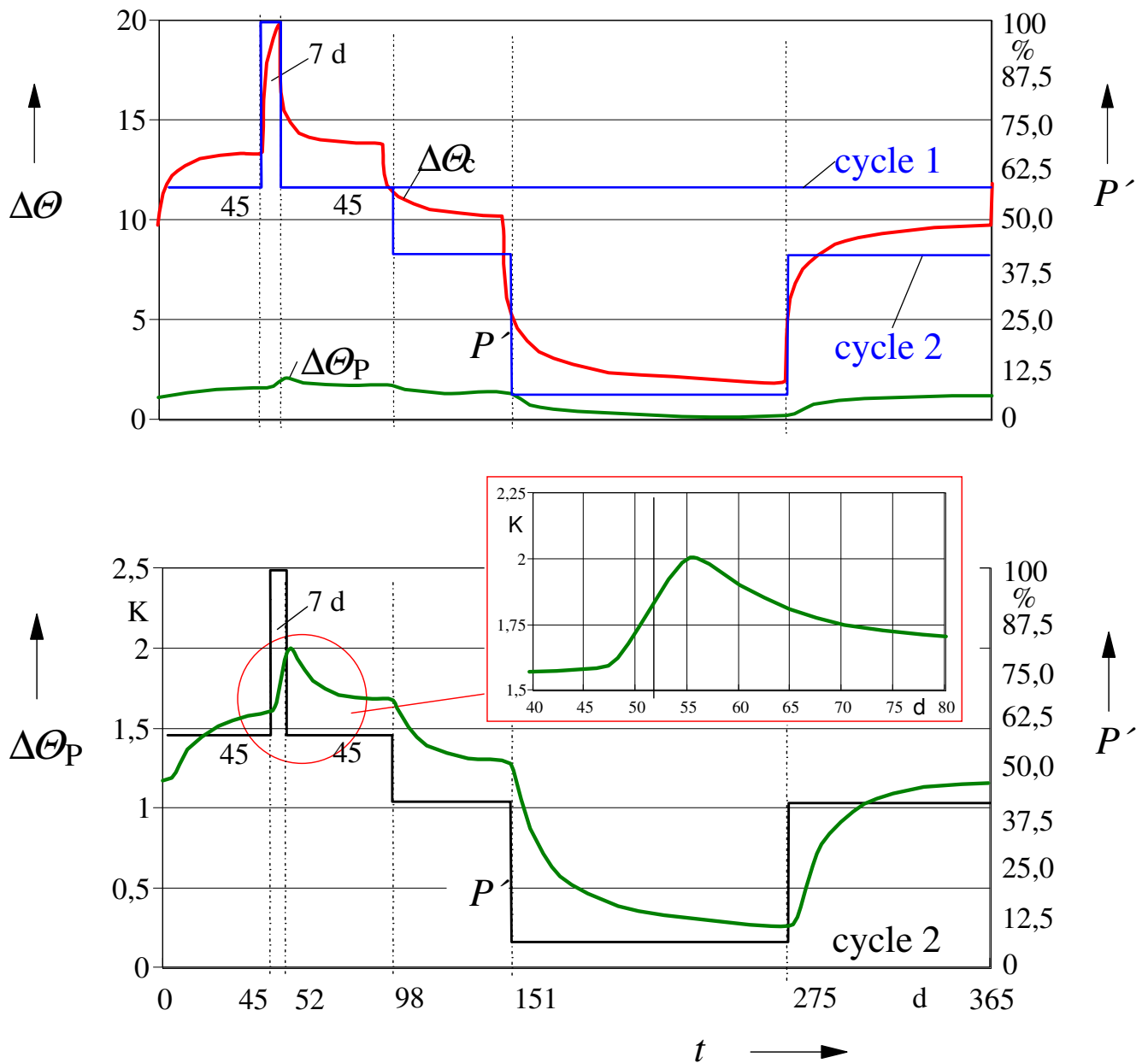


fig. 2: Yearly cycle of cable losses and resulting temperature courses, red: conductor temperature rise $\Delta\Theta_c$; black: temperature rise $\Delta\Theta_p$ of the survey point below: temperature

rise $\Delta\theta_p$ for enlarged scale $h_c = 1.50$ m; $h_p = 0.3$ m; $\hat{P}'_{cab} = 64.8$ W/m; $\lambda = 1.43$ W/(K m); $\theta_a = 12.0^\circ\text{C}$

$\Delta\theta_{d,p}$ in Gl. (6) is the temperature rise of the survey point caused by the dielectric losses P'_d of the cable. With the stationary thermal coupling resistance T'_{CP} between cable and survey point, we get:

$$\Delta\theta_{d,p} = P'_d \cdot T'_{CP} = P'_d \cdot \frac{1}{2 \cdot \pi \cdot \lambda} \cdot \ln \frac{s'_{CP}}{s_{CP}} \quad (8)$$

Equ. (6) is providing the peak value of the conductor losses \hat{P}'_c . From those, unfortunately, the peak value of the current I_p cannot yet be derived, since in the relation

$$\hat{P}'_c = R'_{c20}(\hat{\theta}_c) \cdot I_p^2 = R'_{c20} \cdot \left[1 + \alpha \cdot (1 + (\hat{\theta}_c - 20^\circ\text{C})) \right] \cdot I_p^2 \quad (9)$$

where R'_{c20} ohmic resistance of the conductor for 20°C and α its temperature coefficient

the peak value of the conductor temperature $\hat{\theta}_c$ is still unknown. But this value results directly from

$$\hat{\theta}_c = \theta_a + \hat{P}'_c \cdot \left[T'_{cab} + n \cdot (1 + \lambda_1 + \lambda_2) \cdot T'_{trans,K} \right] + \Delta\theta_{d,K} \quad (10)$$

with the representative thermal resistance of the cable

$$T'_{cab} = T'_1 + n \cdot \left[(1 + \lambda_1) \cdot T'_2 + (1 + \lambda_1 + \lambda_2) \cdot T'_3 \right], \quad (11)$$

and with the conductor temperature rise caused by the dielectric losses

$$\Delta\theta_{d,K} = P'_d \cdot \left[T'_1 / 2 + n \cdot (T'_2 + T'_3 + T'_{trans,K}) \right] \quad (12)$$

The external thermal resistance $T'_{trans,K}$ of the cable in eqs. (10, 12) is calculated again for the given time course of the cable losses $P'(t)$ (with loss steps $\Delta P'_i$ at times t_i) by scanning the time course of the resulting temperature rise and by searching the maximum temperature rise of the cable surface, as this was already done by equ. (7) for the survey point. For a considered point on the cable surface, we get equ. (13):

$$T'_{trans,K} = \frac{1}{\hat{P}'_c} \cdot \text{Max} \left\{ \sum_{i=1}^{n_{\text{step}}} \Delta P'_i \cdot \text{SFR}_{\text{corr}} \right\} \quad (13a)$$

with the thermal step response

$$\text{SFR} = \frac{1}{4 \cdot \pi \cdot \lambda} \cdot \sum_{i=1}^{n_{\text{step}}} \left[\text{E1} \left(\frac{D_{cab}^2}{16 \cdot \delta \cdot (t_x - t_i)} \right) - \text{E1} \left(\frac{h_c^2}{\delta \cdot (t_x - t_i)} \right) \right], \quad (13b)$$

which will be temperature-adapted, as described in the following.

Considering the fact, that the ohmic resistances as well as the losses of the cable will change during the temperature course with changing conductor temperatures, the thermal step

response of equ. (13b) can be modulated by the actual conductor losses. Taking the ohmic conductor resistance at the end of the step response $R'_c(\infty)$ as a basis

$$R'_c(\infty) = R'_{c20} \cdot [1 + \alpha \cdot (\theta_c(\infty) - 20^\circ\text{C})] = R'_{c20} \cdot (1 + \alpha \cdot \Delta\theta_{c,\infty}) \quad (14)$$

and the ohmic conductor resistance at the time t as

$$R'_c(t) = R'_{c20} \cdot (1 + \alpha \cdot \Delta\theta_c(t)) \quad (15)$$

yields the corrected conductor temperature $\theta_{c,\text{corr}}(t)$:

$$\theta_{c,\text{corr}}(t) \approx \theta_c(t) \cdot \frac{R'_{c20} \cdot (1 + \alpha \cdot \Delta\theta_c(t))}{R'_{c20} \cdot (1 + \alpha \cdot \Delta\theta_{c,\infty})} \approx \theta_c(t) \cdot (1 + \alpha \cdot \Delta\theta_c(t)) \cdot (1 - \alpha \cdot \Delta\theta_{c,\infty}) \quad (16)$$

or, in further approximation,

$$\theta_{c,\text{corr}}(t) \approx \theta_c(t) \cdot (1 - \alpha \cdot (\theta_{c,\infty} - \theta_c(t))) \quad (17)$$

From equ. (17) the correction of the conductor temperature given in IEC-publ. 60253 [5] follows:

$$\theta_{c,\text{corr}}(t) \approx \frac{\theta_c(t)}{1 + \alpha \cdot (\theta_{c,\infty} - \theta_c(t))} \quad (18)$$

This correction of the thermal step response is reasonable, since the conductor losses are changing simultaneously with the conductor temperature, thus modulating the corresponding step response. On the other hand, a similar modulation of the temperatures of the survey point seems not to be sensible, as the temperatures of the survey point are reacting on a step of the conductor losses – see for example fig. 2 – with a time delay of at least some days. Therefore, the calculation of the transient thermal coupling resistance $T'_{\text{Trans,P}}$ between survey point P and cable is based on the final value, thus calculating on the safe side.

A further processing of eqs. (6) and (10) results into the rating equation:

$$I_p = \frac{1}{\sqrt{R'_{c\theta}}} \cdot \sqrt{\frac{\Delta\theta_{P,\text{max}} - \Delta\theta_{d,P}}{\underbrace{n \cdot (1 + \lambda_1 + \lambda_2) \cdot T'_{\text{trans,P}}}_{\hat{P}'_c}}} \quad (19a)$$

with the ohmic conductor resistance

$$R'_{c\theta} = R'_{c20} \cdot \left\{ 1 + \alpha \cdot \left[\theta_a - 20^\circ\text{C} + \hat{P}'_c \cdot [T'_{\text{cab}} + n \cdot (1 + \lambda_1 + \lambda_2) \cdot T'_{\text{trans,K}}] + \Delta\theta_{d,K} \right] \right\} \quad (19b)$$

where the peak value of the conductor losses \hat{P}'_c was already determined by equ. (6).

Thus for predefined time courses of the current or of the cable losses, respectively, the foregoing equations (6) and (19) will provide a system, which allows the determination of the current rating by means of a closed equation the shape of which is corresponding with the rating equation in IEC-publ. 60287 [4]. As an additional effort, in a forerun the thermal

transient resistances $T'_{\text{Trans,K}}$ (related to the cable surface) and, in the case of a survey point with temperature limit (e.g. 2 K-criterion), $T'_{\text{Trans,P}}$ as thermal coupling resistance between cable and survey point must be determined.

The current rating I_{02K} of the cable, for the same loss cycle, but without consideration of the 2 K-criterion, follows with the given permissible conductor temperature $\theta_{c,\text{max}}$ to

$$I_{02K} = \frac{1}{\sqrt{R'_{c20} \cdot [1 + \alpha \cdot (\theta_{c,\text{max}} - 20^\circ\text{C})]}} \cdot \sqrt{\frac{\theta_{c,\text{max}} - \theta_a - \Delta\theta_{d,K}}{T'_1 + n \cdot [(1 + \lambda_1) \cdot T'_2 + (1 + \lambda_1 + \lambda_2) \cdot (T'_3 + T'_{\text{trans,K}})]}} \quad (20)$$

The only difference between Gl. (20) and the stationary rating equation in [4] consists in replacing the external thermal resistance of the cable T'_4 by the transient thermal resistance $T'_{\text{trans,K}}$.

Indeed, for calculating the stationary current rating (continuous load) for a cable installation with a temperature-restricted survey point, we get by inserting the stationary thermal resistances:

$$I_P = \sqrt{\frac{1}{R'_c \cdot [1 + \alpha \cdot (\hat{\theta}_c - 20^\circ\text{C})]}} \cdot \sqrt{\frac{\Delta\theta_{P,\text{max}} - \Delta\theta_{d,P}}{\underbrace{n \cdot (1 + \lambda_1 + \lambda_2) \cdot T'_{CP}}_{\hat{P}'_c}}} \quad (21a)$$

$$\text{where } \hat{\theta}_c = \theta_a + \hat{P}'_c \cdot [T'_{\text{cab}} + n \cdot (1 + \lambda_1 + \lambda_2) \cdot T'_4] + \Delta\theta_{d,K} \quad (21b)$$

$$\Delta\theta_{d,K} = P'_d \cdot [T'_1/2 + n \cdot (T'_2 + T'_3 + T'_4)] \quad (21c)$$

3. Example

In this chapter some results from the preceding formulae are discussed for a practical example. Considered is a XLPE-insulated 150-kV-three-core submarine cable with $3 \times 800 \text{ mm}^2$ copper conductors (fig. 3). Some essential parameters of the cable are summarized in table 1.

The cable (outer diameter $D_{\text{cab}} = 218 \text{ mm}$) is laid in a sea floor with a thermal conductivity of $\lambda = 1.43 \text{ W/(K m)}$, and the depth of the survey point is 0.30 m. Current ratings as well as some other results are additionally listed in table 1. Thermal resistances and the loss factors of the conductors, lead sheaths and amour are derived from [4].

For this example, fig. 4 shows the current rating I_{2K} for the application of the 2 K-criterion (green, dotted) and the current rating I_{20K} without the 2 K-criterion (black, dotted) as functions of the laying depth h_c , for the yearly loss cycle 2 of fig. 2 and for the parameters of table 1. The red characteristic curve shows the resulting current rating. As an additional information, the transient thermal resistance $T'_{\text{Trans,K}}$ of the cable as well as the transient thermal coupling resistance $T'_{\text{Trans,P}}$ between survey point P and cable are shown in fig. 5.

The first conclusion from fig. 4 is, that the observance of the 2 K-criterion will lead – especially for smaller laying depths up to 2.5 m – to extensive reductions of the current rating. In the example of table 1 with a laying depth of $h_c = 1.50 \text{ m}$ the current rating will be reduced from $I_{20K} = 959 \text{ A}$ without the 2 K-criterion to $I_{02K} = 681 \text{ A}$, i.e. by approx. 30 %. In the case of $h_c = 1.0 \text{ m}$, the current rating is actually reduced by some 53 %. The current rating of the cable is dominated by the 2 K-criterion for laying depths up to approx. 2.55 m. For farther

enlarged laying depths, the highest permissible conductor temperature of the cable (here: 90°C) rules the current rating

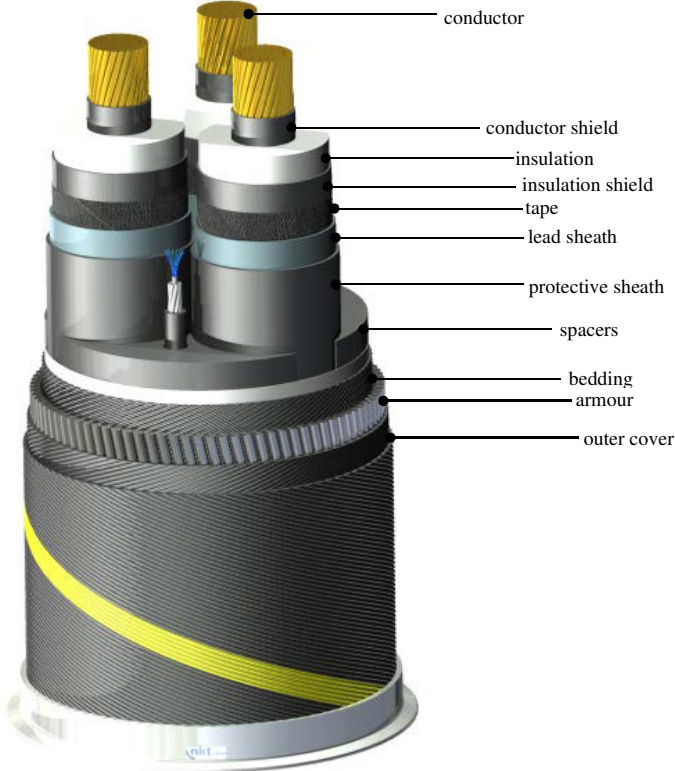


fig. 3: Generic drawing of a 150-kV-submarine cable [source: nkt cables]

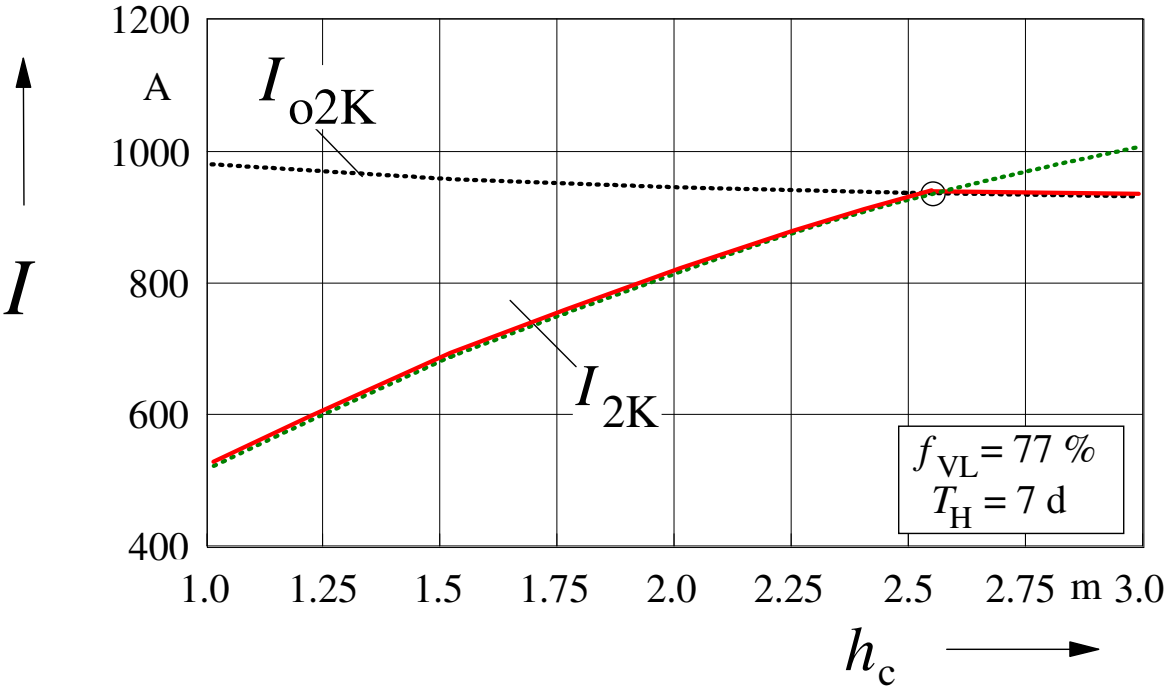


fig. 4: current rating I_{2K} with 2 K-criterion (green) and I_{20K} without 2 K-criterion (black) as well as resulting current rating (red) as functions of the laying depth h_c for the loss cycle 2 in fig. 2 and parameters from table 1

Fig. 6 gives a comparison of the current ratings for three different load cycles. It is elucidated, that for the unrealistic assumption of a continuous load the current rating is extremely reduced against the other current ratings, and that it is dominated by the 2 K-criterion alone. Additionally, it can be realized that (dependent on the laying depth) the special shape of the yearly cycle has a sensible influence on the current rating, - in spite of the long-lasting 45-day phase of preload and the 7-day phase of full load.

This is farther elucidated in fig. 7: here the current ratings from fig. 6 (I_{2K} with 2 K-criterion (green) and I_{20K} without 2 K-criterion (black) for continuous load (red), for cycle 1 (green) and for cycle 2 (black) are faced for the laying depths $h_c = 1.5$ m und $h_c = 2.5$ m. It can be seen, that on the one hand the shape of the loss cycle has an only limited impact on the current rating I_{20K} without 2 K-criterion, whereas on the other hand its influence on the current rating I_{2K} under the 2 K-criterion is quite sensible. This holds especially true for greater laying depths.

	Submarine cable 2X(F)K2YRAA 3*1*800 RM 150/170 kV	unit	value
U_n	nominal voltage	kV	150
n	number of cable cores	-	3
$\Theta_{c,max}$	permissible conductor temperature	°C	90
$R'_{ac,20}$	ohmic conductor-ac-resistance	$\mu\Omega/m$	25.3
α	temperature coefficient	1/K	0.0039
λ_1	loss factor of sheaths	%	25.1
λ_2	loss factor of armor	%	36.4
T_1'	thermal resistance of the electrical insulation	K m/W	0.462
T_2'	thermal resistance of inner protective layers	K m/W	0.132
T_3'	thermal resistance of the armour	K m/W	0.041
T_{cab}	representative thermal resistance of the cable	K m/W	1.156
P_d'	dielectric losses	W/m	3*0,5
D_{cab}	outer diameter of the cable	mm	218
h_c	laying depth	m	1.50
h_p	depth of the survey point	m	0.30
Θ_a	ambient temperature	°C	12
$\Delta\Theta_{P,max}$	highest permissible temperature rise of survey point P	K	2.0
$\Delta\Theta_{d,P}$	temperature rise of survey point by dielectric losses	K	0.10
λ	thermal conductivity of the soil	W/(K m)	1.43
δ	thermal diffusion coefficient	m^2/s	$6.23 \cdot 10^{-7}$
T_4'	external thermal resistance of the cable	K m/W	0.369
T_{cP}'	coupling thermal resistance of the cable – survey point	K m/W	0.045
$T_{Trans,P}'$	transient value of T_{cP}' for cycle 2	K m/W	0.031
$T_{Trans,K}'$	transient value of T_4' for cycle 2	K m/W	0.305
I_p	current rating with 2 K-criterion	A	681
$\hat{\Theta}_c$	maximum conductor temperature for I_p	°C	46.0
I_{02K}	current rating without 2 K-criterion	A	959

table 1: Parameters of the example

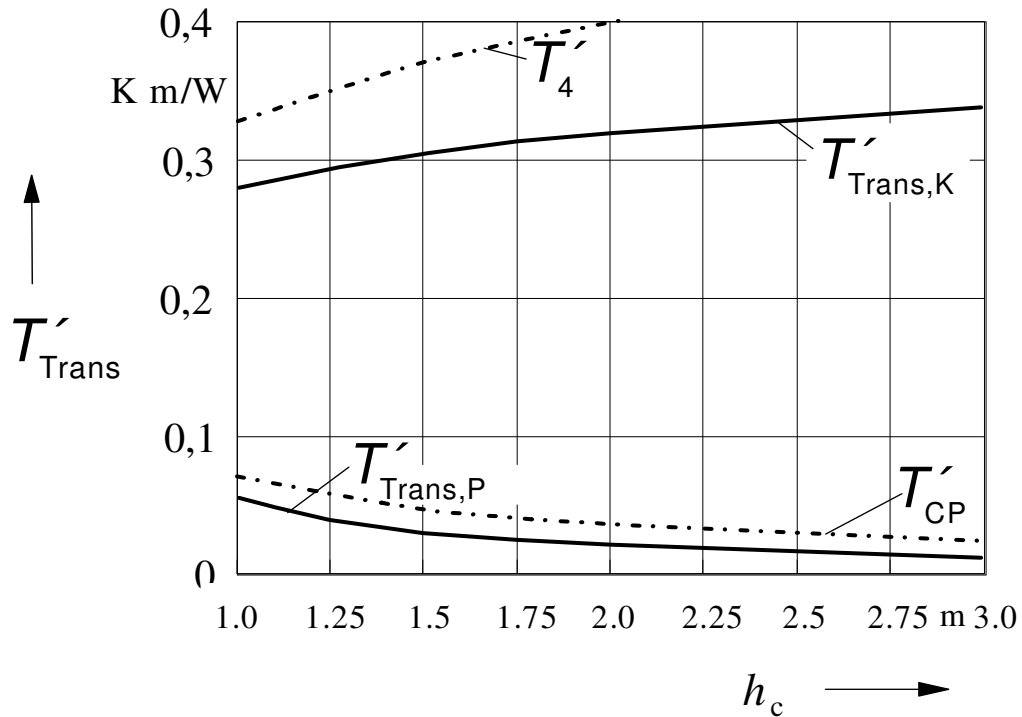


fig. 5: transient thermal resistances as functions of the laying depth h_c chain line: corresponding stationary values

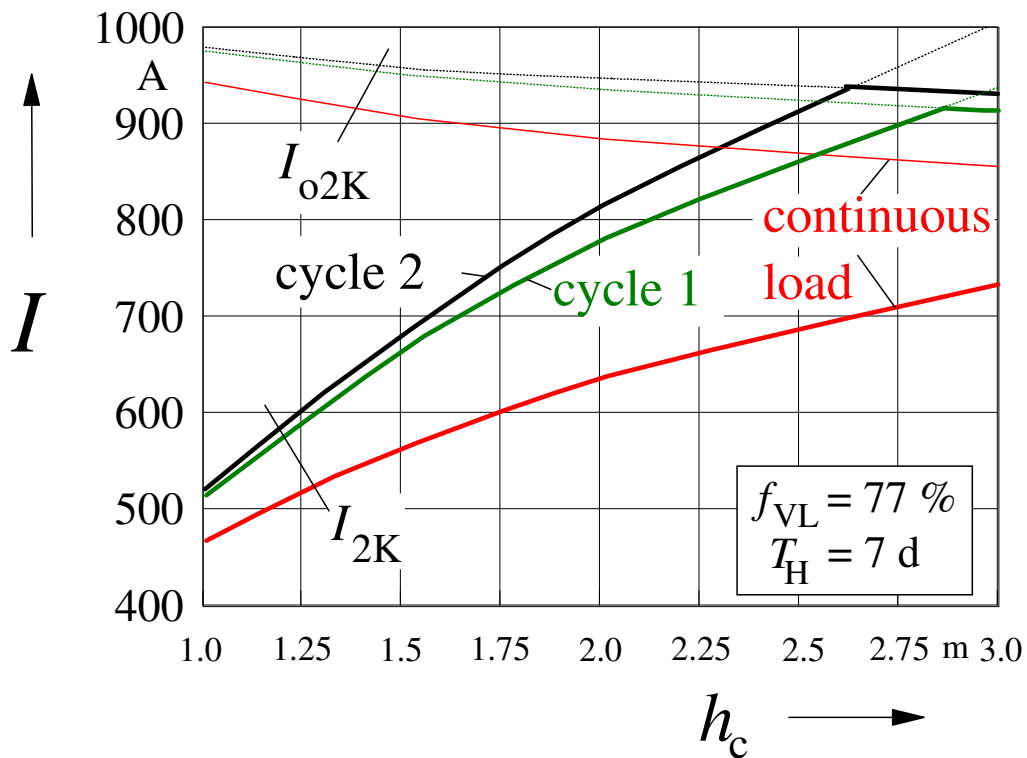


fig. 6: current rating I_{2K} with 2 K-criterion (green) and I_{20K} without 2 K-criterion (black) for continuous load (red) as well as for cycle 1 (green) and for cycle 2 (black) from fig. 2, as functions of the laying depth h_c and for parameters from table 1

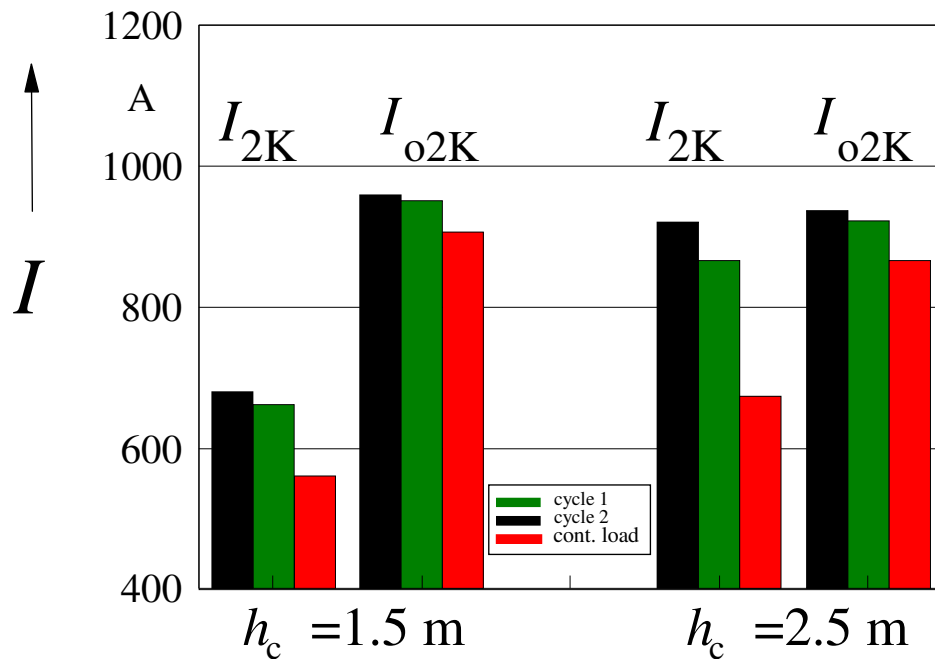


fig. 7: current rating I_{2K} with 2 K-criterion (green) and I_{2oK} without 2 K-criterion (black) for continuous load (red), for cycle 1 (green) and for cycle 2 (black) from fig. 2 and for parameters from table 1, for two laying depth h_c

3. Conclusions

In some actual cases, the given trends towards an enlargement of the maximum power of existing windparks (key words: Power Boost and Repowering) are requesting a higher load for the existing export cables. Thus, the described calculation method may be of interest for the analysis of such possibilities.

But for the in-depth investigation of such possibilities several different aspect are to be considered, from which the 2 K-criterion is only one aspect. Very important is the consideration of the fact, that the loss factors of the lead sheaths and the armour of submarine cables are estimated by IEC-publ 60287 [4] by far too high, -a nowadays internationally accepted fact. Therefore, sophisticated computation models of the cable construction for an improved simulation of the thermal/electromagnetic behavior of the submarine cable are requested. Further aspects are the consideration of the load reduction because of windpark losses and reduced availability of the windmills. Another possibility is a refined modeling of the seabed. A future publication [8] will discuss these problems and possibilities in detail.

Moreover, in the future for onshore cable routes, too, such restrictions of soil heating by cables are imaginable. Besides ecological restrictions further examples of temperature restrictions can be given in the case of adjacent infrastructural lines, as e.g. pipes for gas, water etc.

4. References

- [1] BSH: Konstruktive Ausführung von Offshore-Windenergieanlagen German Maritime and Hydrographic Agency (BSH), Juni 2007
- [2] BMU: Ökologische Auswirkungen von 380-kV-Erdleitungen und HGÜ-Erdleitungen, Federal Ministry for the Environment, Nature Conservation, Buildings and Nuclear Safety, FKZ 03MAP189, Berlin 2011
- [3] H. Brakelmann, F. Richert: Bemessung der Energiekabel zur Netzanbindung on Offshore- Windfarmen“, El.wirtsch. 103 (2004), pp. 56-59
- [4] IEC: Electric cables – Calculation of the current rating Part 1-1: Current rating equation (100 % load factor) and calculation of losses, IEC-Publ. 60287-1-1, Paris, second edition, 2006-12
- [5] IEC: Calculation of the cyclic and emergency current rating of cables. Part 2: Cyclic rating of cables greater than 18/30 (36) kV and emergency ratings for cables of all voltages”, IEC-Publ. 60853-2, 1989
- [6] M. Abramowitz, I.A. Stegun: Handbook of Mathematical Functions, Dover-Publ., New York, 1970
- [7] H. Brakelmann: Energietechnik programmiert, Probleme, Lösungen, Programme, VDE-Verlag (1989), pp. 1 - 266
- [8] H. Brakelmann, J. Stammen, e.a.: „Mögliche Belastungssteigerungen bei bestehenden Exportkabeln von Offshore-Windparks, to be published